Optimal Duplex Mode Selection for D2D-Aided Underlaying Cellular Networks

Changhao Du, Zhongshan Zhang, *Senior Member, IEEE*, Xiaoxiang Wang, and Jianping An, *Member, IEEE*

***Abstract*—Both Device-to-device (D2D) and full-duplex (FD) have been widely recognized as spectral efficient techniques in the fifth-generation wireless communications systems. By enabling FD mode in D2D communications, the attainable spectrum efficiency can be (in theory) up to twice as high as that of conventional half-duplex (HD) mode D2D technology, provided that the self-interference signal in the former can be sufficiently suppressed. Considering the fact that FD technology does not always outperform the HD technology in arbitrary channel condition, we will delve into the FD gain as well as its preconditions for acquisition in this paper. In particular, the performance of D2D-aided underlaying cellular networks is investigated by assuming that the D2D users are capable of operating at both HD and FD modes. Under a given user workload, the sum throughput in each DU is shown to be always improved by activating D2D links despite an extra DU-induced interference could be imposed on its co-spectrum cellular users. Numerical results show that the FD-D2D mode exhibits its superiority in terms of sum throughput than the HD-D2D mode in a light-workload scenario even if a non-ideal SI cancellation has been implemented in the former, but the latter pulls back a game in a heavy-workload scenario. Furthermore, to maximize the sum throughput, an appropriate mode-selection scheme (i.e., by choosing either FD or HD mode in the current time-slot for each individual D2D user) should be implemented for sufficiently exploiting the FD gain according to the instantaneous radio frequency environment.**

***Index Terms*—Device-to-Device, full-duplex, underlaying cellular networks, average coverage probability, occupation probability.**

I. Introduction

With the rapid development of new technologies such as the Internet of Things as well as the rapid popularization of new services such as high-definition video on demand, wireless spectrum resources are becoming increasingly scarce. To meet the growing communication demands of customers, the spectral efficiency of the existing wireless networks must be substantially improved [1]–[5]. Meanwhile, the base stations (BSs) under the conventional BS-centric cellular network architecture may often operate at an overloaded status (especially in a rush hour), thus resulting in a severe load imbalance over the network [6].

Device-to-device (D2D) technology, which allows the geographically neighboring devices to communicate directly without relying on the involvement of BSs, has been regarded as one of the core techniques of the fifth-generation (5G) wireless communications systems that will provide an unprecedented quality of service to the customers [7]–[9]. Several advantages, including a significantly improved throughput [10], an improved spectral efficiency [11], [12], an extended radio coverage of mobile users [13], a reduced power consumption in mobile devices [14], [15], a lower end-to-end latency [16], and an efficaciously relieved traffic budget from the BS side to the terminal side [17], etc, have been exhibited in D2D technology. In particular, unlike the conventional cellular users (CUs), path loss due to the large-scale fading between D2D users (DUs) can be substantially relieved due to the fact that the distance between D2D pairs is usually much less than the CU-to-BS distance.

Besides D2D, the full-duplex (FD) technology has also been regarded as an appealing technology with a great potential for improving the spectrum efficiency in 5G systems [18]. Since the FD-mode users are allowed to perform concurrent transmission and reception over a single spectrum,[1] the FD gain in terms of the attainable spectral efficiency over the half-duplex (HD) mode can (in theory) be up to twice [19]–[21]. Although the HD mode has already been widely adopted in the existing D2D communication networks [22], the spectral efficiency of the D2D-aided underlaying cellular networks (CNs) can definitely be further improved by employing FD technology.

A. Motivation

Although D2D has been proven to be a spectral-efficient technology, there still exist some bottlenecks to overcome in D2D-aided underlaying CNs, such as (just list a few of the most typical issues)

Manuscript received June 2, 2019; revised October 31, 2019 and December 25, 2019; accepted January 14, 2020. Date of publication January 28, 2020; date of current version March 12, 2020. This work was supported in part by the Key Project of the National Natural Science Foundation of China under Grant 61431001 and in part by the Key Laboratory of Cognitive Radio and Information Processing, Ministry of Education (Guilin University of Electronic Technology), and Beijing Institute of Technology Research Fund Program for Young Scholars. The review of this article was coordinated by Dr. D. Marabissi. *(Corresponding author: Zhongshan Zhang.)*

C. Du is with the Beijing University of Posts and Telecommunications, Key Laboratory of Universal Wireless Communications, Ministry of Education, Beijing 100876, China, and also with the School of Information and Electronics, Beijing Institute of Technology, Beijing 100081, China (e-mail: changhao.du@bupt.edu.cn).

Z. Zhang and J. An are with the School of Information and Electronics, Beijing Institute of Technology, Beijing 100081, China (e-mail: zhangzs@bit.edu.cn; an@bit.edu.cn).

X. Wang is with the Beijing University of Posts and Telecommunications, Key Laboratory of Universal Wireless Communications, Ministry of Education, Beijing 100876, China (e-mail: cpwang@bupt.edu.cn).

Digital Object Identifier 10.1109/TVT.2020.2968053

[1] Without loss of generality, we use FD mode D2D technology as an example to explain the technical advantages of FD. In this scenario, the licensed spectrum that has been allocated to a conventional CU is allowed to be reused by a pair of DUs.

1) The DUs typically reuse the licensed spectrum that has already been allocated to the conventional CUs, in which case the D2D transmitters (DTs) may impose a severe interference on the co-spectrum CUs whenever both of them are activated simultaneously. Evidently, the D2D-induced interference may significantly erode the performance of conventional CUs [23], [24].
2) The amount of traffic load (which is also referred to as "workload") carried on each user can be used for characterizing the user's current working status (i.e., in silence or active status). On the one hand, users with a heavier workload will take longer on the spectrum, which will inevitably cause long-term interference to other users. On the other hand, under the premise of a given peer-to-peer traffic load, the active communication cycle of DUs in FD mode (FD-DUs) will be reduced to half of the DUs in HD mode (HD-DUs) (i.e., once the current workload is sent, the node must go to the silence status immediately to avoid imposing a further interference on the other users).
3) Although FD technology usually outperform HD technology in terms of spectral efficiency, the severe self-interference (SI), which happens between the transmit and receive antennas of the same FD device, may totally drown out the signal of interest that is transmitted by a remote transmitter [25]. Consequently, the SI may erode the attainable FD gain or even lead to a performance worse than the conventional HD technology. Although most of the SI power can be sufficiently suppressed by employing an appropriate SI cancellation (SIC) technique (please refer to [19] for details), the residual SI (RSI) may still erode the FD gain to some extent.
4) In each transmission of DUs, either FD or HD mode can be employed, subjecting to the maximization of the sum throughput of the underlaying CNs. Since FD does not always outperform HD, each DU must be capable of adaptively choosing an appropriate duplex mode according to its current channel quality.

To address the above issues, the optimal FD/HD mode selection in the underlaying CNs must be performed for maximizing the attainable performance gain.

B. The Existing Work

The performance analysis of the D2D-aided underlaying CNs has been widely carried out. For instance, a closed-form expression for the average coverage probability (ACP) of the underlaying CNs has been derived in [26], where the authors gave out an analytic expression for the ACP of the CUs relying on both stochastic geometry and Poisson point process (PPP). However, the authors in [26] failed to derive the closed-form expression for the ACP of the D2D-links (DLs). In order to address the above-mentioned issue, the authors in [27] derived the expressions for the ACP of both the conventional cellular-links (CLs) and the DLs, however, without considering the impact of the inter-CU interference. In [28], the authors developed the general models for the signal-to-interference-plus-noise ratio (SINR) in multi-cell scenarios by employing the theory of stochastic geometry. Following the SINR analysis, the authors also obtained the closed-form expressions for a variety of critical performance metrics, including the mean data rate and the mean rate losses under static-frequency reuse conditions. However, the impact of co-cell CUs' distribution on the average data rate was still not analyzed in [28]. In [29], [30], the authors investigated the impacts of both spatial densities and transmit power allocation ratio on the achievable transmission rate by considering both dual-band and multi-bands scenarios. In [31], the closed-form expressions for both the ACP and the sum data rate of underlaying CNs were derived by taking the impact of inter-user interference into account. In addition, in [32], the tight throughput bounds of FD mode based networks were derived by considering the break point in the attainable performance gain of the networks.

Based on the above research progress, the academia/industry have proposed a variety of mode selection schemes for the underlaying CNs. For example, an optimal mode selection scheme in terms of success-transmitter-probability maximization has been proposed for protecting the communication quality of the primary user [33], in which both the interference and position were concerned. In addition, a mode-selection scheme in terms of sum-capacity maximization has been proposed in [34], where the inter-user interference was treated.

Despite all this, the impact of DUs' workload on either the ACP or the sum throughput was rarely considered in the existing work. For instance, the authors in [31]–[34] failed to consider the impact of workload distribution on either ACP or sum throughput, let alone the difference between the employment of FD-DUs and the implement of HD-DUs (note that the average interference intensity of the activated FD-DUs is twice that of the activated HD-DUs). In the following, let us temporarily ignore the impact of RSI on the FD mode. Meanwhile, a scenario of symmetric transmission (i.e., D2D pairs each has the same amount of data to exchange with each other) will be considered. In this case, the average active period of the FD-DUs can be compressed to half of the average active period of the HD-DUs. In other words, although the FD-DUs may have a higher interference intensity than the HD-DUs during the active period, the data transmission of the former can be quickly completed, thereby upgrading the second half of the saved time to an interference-free period for the co-spectrum CUs. By exploiting this benefit, a higher sum throughput can be obtained in the FD-DUs aided underlaying CNs than in the HD-DUs aided underlaying CNs. In summary, as far as we know, mode selection technique in terms of sum-throughput maximization of the underlaying networks has not been sufficiently investigated by considering the impact of the workload in each user.

C. The Proposed Technological Approaches

In order to balance the performance gain between FD-DUs and HD-DUs, the technique for switching between HD and FD mode may constitute a major concern of the proposed D2D-aided underlaying CNs. Note that the D2D-induced interference will always be imposed on the co-spectrum CUs whenever the DUs (either HD-DUs or FD-DUs) are activated, the CUs' SINR will

always be eroded. To reduce the above-mentioned performance loss, the DUs must compress their active duration as much as possible, provided that their workload (i.e., the data to transmit/exchange) can be completed within this duration. As a rule, for a given data block to be exchanged between a pair of DUs, the DT must switch to the silence state once it completes the whole data transmission for the purpose of mitigating an unnecessary interference on its co-spectrum CUs.

By employing FD-DUs, the D2D-induced interference duration can be reduced to half of that of HD-DUs.[2] For instance, given a pair of DUs that are going to exchange their data blocks, we may assume that the data blocks held by these two DUs are of the same volume. Basically, two equal-length time slots are needed for these two HD-DUs to exchange their data blocks, allowing one and only one DU to transmit in each time slot (the role of these two DUs will exchange in the next time slot). In other words, the whole duration of two time slots can be regarded as D2D-induced interfering period when HD-DUs are considered. Unlike HD-DUs, the interfering time can be suppressed to one-time-slot duration by employing FD-DUs due to the capability of simultaneous transmission and reception in each DU. Although the active FD-DUs will produce a much stronger interference to the co-spectrum CUs than the activating HD-DUs, this FD-interference period will end soon, leaving the remaining time to be in zero-interference state. For this reason, FD-DUs will be more conducive to improving the sum throughput of the proposed underlaying CNs.

D. Main Contributions

In this paper, the benefit brought about by employing D2D technique in underlaying CNs will be analyzed, with the closed-form expressions for both ACP and sum throughput derived by taking the impact of the users' workload into account. We consider a multi-cell scenario, in which both HD-DUs and FD-DUs can be implemented. Furthermore, each DU is assumed to be capable of adaptively switching its duplex mode between FD and HD according to the instantaneous channel quality so as to optimize the sum throughput. Without loss of generality, a set of (co-cell) users (comprising N_c CUs and N_d DUs) are allowed to share the same spectrum resource according to a homogeneous PPP model. The main contributions of this paper are reflected in the following aspects:

1) The workload of each user can be quantized by the activated probability (AP). Meanwhile, to quantitatively characterize the silence or working status of each user, the concept of "occupation probability (OP)" together with AP can be employed.
2) Based on the OP of each user, the closed-form expressions of ACP for both CLs and DLs are derived by considering the impact of both cross-interference and RSI between CUs and DUs.
3) The closed-form expressions of sum throughput for both FD-D2D-aided underlaying CNs (FNs) and HD-D2D-aided underlaying CNs (HNs) are derived.
4) The break point corresponding to the maximum sum throughput for both FNs and HNs can be used as the basis for FD/HD mode selection.
5) Finally, the performance of underlaying CNs employing either FD or HD mode will be compared and analyzed via simulation. The impacts of a variety of parameters, including the average workload, the RSI, the SINR threshold and the density of activated users (AUs), etc, on the sum throughput will be investigated.

The remainder of this paper is organized as follows. In Section II, the system model for the proposed underlaying CNs is described. The received SINRs for both FD-DUs and HD-DUs are analyzed in Section III, followed by deriving both the successful transmission probability (STP) and ACP of CUs and DUs in Sections IV and V, respectively. After that, sum throughput as well as break point of the proposed underlaying CNs by employing the optimal duplex mode will be evaluated in Section VI. Furthermore, numerical results are given out by Section VII. Finally, Section VIII concludes this paper.

Notation: $\mathbb{P}$ represents the probability of an event, and $\mathcal{P}$ denotes the transmit power of an activated user. Furthermore, $\mathcal{S}$ and $\mathcal{T}$ stand for the STP and throughput of a wireless link, respectively. Moreover, $\mathcal{L}$ denotes the Laplace transforms of a random variable. In addition, $\mathbb{E}$ is used to denote the expectation operation. Finally, $({}_pF_q)(\cdot)$ denotes the generalized hypergeometric function. A list of symbols that employed in this paper is given by Table I.

II. System Model

Following the concept of AP, which is usually used for characterizing the probability that a DU can be activated, the volume of traffic that exchanged between D2D pairs can be measured by employing a new concept called OP. The D2D-aided CNs can thus be modelled by employing the above concepts. Furthermore, whether the co-spectrum CLs and DLs are allowed to be activated simultaneously or not will be considered in the proposed model, with totally five scenarios investigated, including: (i) only CLs are activated; (ii) only FD mode DLs are activated; (iii) only HD mode DLs are activated; (iv) both CLs and FD mode DLs are activated simultaneously; (v) both CLs and HD mode DLs are activated simultaneously.

A. Some Basic Definitions

1) Interference in D2D-Aided Underlaying Cellular Networks: According to the existing standards such as ProSe [35], the uplink licensed spectrum (already allocated to the cellular networks) is allowed to be reused by the D2D links. Therefore, in this reuse-spectrum scenario, we will focus on the interference in the uplink.

Let us consider a BS-centric cell, in which the D2D mode is enabled in some terminals, as illustrated in Fig. 1. By employing

[2]Of course, this conclusion can be strictly validated in scenarios comprising only a single D2D pair. In the presence of multiple D2D pairs, on the other hand, the D2D-induced interference becomes much more complicated and we are almost impossible to get the concise "half-duration" equality between FD-DUs and HD-DUs. Anyway, when D2D pairs are loosely distributed throughout the network (i.e., different D2D pairs are separated far enough apart to make the mutual interference be negligible), the above statement is still valid.

TABLE I
LIST OF SYMBOLS

Symbol	Definition
G_C	The traffic density of CUs
G_D	The traffic density of DUs
$\mathbb{P}[k]$	The probability that a user generate k packets in a period
$\mathbb{P}_{ac}$	The probability that a CU is activated in a time slot
$\mathbb{P}_{ad}$	The probability that a DU is activated in a time slot
$\mathbb{P}_c$	The probability that a time slot is occupied by a CU
$\mathbb{P}_h$	The probability that a time slot is occupied by a HD-DU
$\mathbb{P}_f$	The probability that a time slot is occupied by a FD-DU
Φ_b	PPP to constitute BSs
Φ_c	PPP to constitute CUs
Φ_d	PPP to constitute DUs
λ_b	The density of BSs
$\hat{\lambda_c}$	The density of CUs
$\hat{\lambda_d}$	The density of DUs
λ_c	The density of activated CUs
λ_d	The density of activated DUs
$\mathcal{P}_c$	The transmit power of CUs
$\mathcal{P}_d$	The transmit power of DUs
$\mathcal{P}_{ij}$	The received power at j transmitted by i
h_{ij}	The channel fading coefficient between i and j
d_{ij}	The distant between i and j
R	The maximum cellular link distance
R_d	The average D2D link distance
I_{RSI}	The power of residual self-interference
μ	The self-interference cancellation coefficient
α	The standard path loss exponent
σ^2	The noise power
N_c	The number of activated CUs in a BS-centered cell
N_d	The number of activated DUs in a BS-centered cell
ϵ	The SINR threshold
r_c	Generic cellular link distance

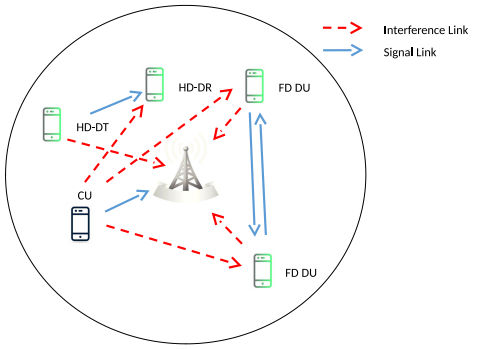

Fig. 1. The interference generated in a D2D-aided cell.

the FD-D2D mode, the BS will suffer from the interference caused by DUs (of course, each CU will also impose interference on its co-spectrum FD-DUs). Unlike FD-D2D mode, in which all the activated D2D pairs will impose interference on both BS and their co-spectrum CUs, and vice versa, the BS suffers from interference induced only by the HD-mode DT, meanwhile the co-spectrum CUs will impose interference on only the HD-mode D2D receiver (DR).

2) Occupation Probability: To analysis the sum throughput under variant traffic densities, some hypotheses should be made firstly. In each user (either a CU or a DU), the probability that k (source data) packets are generated during a given period, in which G frames are expected, is given by the Poisson distribution:

$$\mathbb{P}[k] = \frac{G^k e^{-G}}{k!}. \tag{1}$$

In the following, G is used to denote the traffic density. Therefore, the probability of "NO TRAFFIC IS GENERATED" can be expressed as e^{-G}. If a user has data to transmission, it will keep activation until the data transmission is completed. The probabilities that a CU and a DU are activated can thus be expressed as $\mathbb{P}_{ac} = 1 - e^{-G_C}$ and $\mathbb{P}_{ad} = 1 - e^{-G_D}$, respectively, where G_C and G_D denote the traffic densities of CUs and DUs, respectively.

In this part, we employ OP rather than AP to measure a user's workload. In particular, a user's OP can be used to define its occupation of a time slot, as measured by using the product of AP and the ratio of interactive-data-duration to the whole time slot duration. For a two-time-slot duration, a pair of HD-DUs will occupy the whole duration for exchanging their data, while only one time slot is required for a pair of FD-DUs to complete their data exchange.

In the following, we assume that all the CUs have the same amount of traffic to transmit, meanwhile all the DUs have the same workload (but the a DU's workload is not necessarily equal to that of a CU). Thus the OPs for CUs, HD-DUs and FD-DUs can be expressed as $\mathbb{P}_c = 1 - e^{-G_C}$, $\mathbb{P}_h = 1 - e^{-G_D}$ and $\mathbb{P}_f = (1 - e^{-G_D})/2$, respectively.

B. System Model for D2D-Aided Underlaying CNs

In the D2D-aided underlaying CNs, the BSs, CUs and DUs are assumed to be distributed within a given area according to homogeneous PPP models Φ_b, Φ_c and Φ_d of densities λ_b, $\hat{\lambda_c}$ and $\hat{\lambda_d}$, respectively. The network is assumed to be capable of offering services to a group of users (including both CUs and DUs) simultaneously. In particular, a BS-centered cell (as shown in Fig. 1) is assumed to be capable of supporting N_c CUs as well as N_d DUs, allowing the maximum allowable CU-to-BS distance of R. Meanwhile, the average DT-to-DR distance is assumed to be R_d. In the following, a pair of D2D pairs will be marked by $(x_i, m(x_i)) \in \Phi_d$, in which both $\| x_i - m(x_i) \| = R_d$ and $m(x_i) = x_i + R_d(\cos\varphi_i, \sin\varphi_i)$ are satisfied, and the parameter φ_i is assumed to be independently and uniformly distributed (i.i.d.) in $[0, 2\pi)$.

By using $\mathcal{P}_{ij}$ to represent the received signal power at user j that is transmitted by user i, we get

$$\mathcal{P}_{ij} = \mathcal{P}_i h_{ij} d_{ij}^{-\alpha}, \tag{2}$$

where $\mathcal{P}_i$ represents the transmit power of user i, while h_{ij} denotes the exponentially distributed channel fading coefficient between the transmitter i and the receiver j, and d_{ij} stands for the distance between transmitter i and receiver j. In particular, by expressing the average power of thermal noise as σ^2, the average RSI power of FD-DUs after performing SIC (i.e., I_{RSI}) can be given by $I_{\mathrm{RSI}} = \mathcal{P}_d/\mu$, where μ denotes the SIC coefficient.[3] Furthermore, α is used to express the standard path loss exponent subjecting to the constraint $\alpha > 2$. In addition, all the wireless

[3] A higher SIC coefficient corresponds to a higher SI cancellation capability.

links (as denoted by $h_{ij} \backsim \exp(1)$, where $i, j \in \Phi_b, \Phi_c, \Phi_d$) are assumed to be i.i.d. variables according to the above-mentioned model. In the following, without loss of generality, a constant transmit power is assumed in each CU/DU.

III. Received SINR at Both CLs and DLs

In each time slot, the DLs can be activated as requested, provided that a tolerable performance can be maintained at the co-spectrum CLs. Basically, we have two choices for the links' activation:

1) The co-spectrum CLs and DLs *can be* activated simultaneously;
2) The co-spectrum CLs and DLs *are not allowed* to be activated simultaneously. In order to prevent the reader from disambiguating the above discussion, we explain this as follows: once the CLs are activated, the co-channel DLs must remain inactive, and vice versa; of course, multiple CLs or multiple DLs are still allowed to be activated at the same time.

Evidently, there exists no cross-interference between CLs and their co-spectrum DLs in the latter case. By assuming that the distribution of the AUs follows the PPP model, where the densities of CUs and DUs can be expressed by $\hat{\lambda}_c$ and $\hat{\lambda}_d$, respectively, each user (either CU or DU) can be independently activated according to its instantaneous communication task. Therefore, the activated CUs (ACUs) and activated DUs (ADUs) are distributed according to homogeneous PPP variables Π_c and Π_d of densities $\lambda_c = \mathbb{P}_{ac} \cdot \hat{\lambda_c}$ and $\lambda_d = \mathbb{P}_{ad} \cdot \hat{\lambda_d}$, respectively.

A. Co-Spectrum CLs and DLs Are Not Activated Simultaneously

In this case, there exists no cross-interference between ACUs and ADUs. The received SINR conceived by variant users, including ACUs,[4] FD-ADUs and HD-ADUs, can be expressed:

$$\begin{cases} \mathrm{SINR}_c^{(\mathrm{ND})} = \dfrac{\mathcal{P}_{c_0 b}}{I_{cc} + \sigma^2} \\ \mathrm{SINR}_d^{(\mathrm{FC})} = \dfrac{\mathcal{P}_{dd}}{I_{dd}^{(\mathrm{FD})} + \sigma^2 + I_{\mathrm{RSI}}} \\ \mathrm{SINR}_d^{(\mathrm{HC})} = \dfrac{\mathcal{P}_{dd}}{I_{dd}^{(\mathrm{HD})} + \sigma^2} \end{cases} \tag{3}$$

respectively, where the inter-ACU-interference can be expressed by $I_{cc} = \sum_{c_i \in \Pi_c / c_0} \mathcal{P}_{c_i b}$ with c_i denoting the i-th ACU within Π_c. Furthermore, $I_{dd}^{(\mathrm{FD})} = \sum_{x_i \in \Pi_d / x_0} [\mathcal{P}_{x_i d} + \mathcal{P}_{m(x_i) d}]$ is used to represent the interference among FD-ADUs and $I_{dd}^{(\mathrm{HD})} = \sum_{x_i \in \Pi_d / x_0} \mathcal{P}_{x_i d}$ stands for the interference among HD-ADUs, where x_i and $m(x_i)$ constitute the i-th D2D pair with Π_d. In addition, we may use subscript "0" instead of i to specify the AU in the cell of interest.

[4]We label it by using superscript "ND," because there exists no interference imposed by DUs. Similarly, we label FD-ADUs and HD-ADUs by superscripts "FC" and "HC," respectively, because there exists no interference imposed by CUs.

B. Co-Spectrum CLs and DLs Are Activated Simultaneously

In the sequel, let us express the received SINR for both FD-ADUs and HD-ADUs:

1) *For HD-DUs:* The received SINR at CUs and DUs can be expressed:

$$\begin{cases} \mathrm{SINR}_c^{(\mathrm{HD})} = \dfrac{\mathcal{P}_{c_0 b}}{I_{dc}^{(\mathrm{HD})} + I_{cc} + \sigma^2} \\ \mathrm{SINR}_d^{(\mathrm{HD})} = \dfrac{\mathcal{P}_{dd}}{I_{cd} + I_{dd}^{(\mathrm{HD})} + \sigma^2} \end{cases} \tag{4}$$

respectively, where $I_{dc}^{(\mathrm{HD})} = \sum_{x_i \in \Pi_d / x_0} \mathcal{P}_{x_i b}$ denotes the interference imposed on CUs by its co-spectrum HD-ADUs, and $I_{cd} = \sum_{c_i \in \Pi_c / c_0} \mathcal{P}_{c_i d}$ stands for the interference imposed on ADUs by their co-spectrum ACUs.

2) *For FD-DUs:* The received SINR at CUs and DUs can be expressed:

$$\begin{cases} \mathrm{SINR}_c^{(\mathrm{FD})} = \dfrac{\mathcal{P}_{c_0 b}}{I_{dc}^{(\mathrm{FD})} + I_{cc} + \sigma^2} \\ \mathrm{SINR}_d^{(\mathrm{FD})} = \dfrac{\mathcal{P}_{dd}}{I_{cd} + I_{dd}^{(\mathrm{FD})} + \sigma^2 + I_{\mathrm{RSI}}} \end{cases} \tag{5}$$

respectively, where $I_{dc}^{(\mathrm{FD})} = \sum_{x_i \in \Pi_d} [\mathcal{P}_{x_i b} + \mathcal{P}_{m(x_i) b}]$ represents the interference imposed on CUs by their co-spectrum FD-DUs.

IV. Successful Transmit Probability of CLs and DLs

The STP of a randomly chosen link can be defined by the probability that the quality of this link reaches its predetermined SINR threshold ϵ. We may express this by using $\mathcal{S} = \mathbb{P}(\mathrm{SINR} > \epsilon)$. In the following, by employing an identical ϵ in all scenarios, we can express the STP of both CUs and DUs for each case that was considered in Section III:

$$\begin{cases} \mathcal{S}_c^{(\dagger)} = \mathbb{P}\left(\mathrm{SINR}_c^{(\dagger)} > \epsilon\right) \\ \mathcal{S}_d^{(\ddagger)} = \mathbb{P}\left(\mathrm{SINR}_d^{(\ddagger)} > \epsilon\right) \end{cases} \tag{6}$$

where $\dagger \in \{\mathrm{ND}, \mathrm{HD}, \mathrm{FD}\}$ and $\ddagger \in \{\mathrm{HC}, \mathrm{FC}, \mathrm{HD}, \mathrm{FD}\}$. Next, let us derive the closed-form expression for each case.

A. CLs and Co-Spectrum DLs Are Not Activated Simultaneously

1) CLs are Activated Alone: If no DU is allowed to be activated during the period that its co-spectrum ACUs are communicating, the interference contributed by only CLs should be considered in expressing the SINR. In this case, based on (6), the STP of CLs can be calculated:

$$\begin{aligned} \mathcal{S}_c^{(\mathrm{ND})} &= \mathbb{P}\left(\frac{\mathcal{P}_c h_{c_0 b} d_{c_0 b}^{-\alpha}}{I_{cc} + \sigma^2} > \epsilon\right) \\ &= \int_0^R \left[\mathcal{L}\left(s_c I_{cc}\right) e^{-s_c \sigma^2} f(r_c)\right] dr_c \end{aligned} \tag{7}$$

where $s_c = \epsilon r_c^{\alpha}/\mathcal{P}_c$, $r_c = d_{c_0 b}$. $\mathcal{L}(s_c I_{cc})$ denotes the Laplace transform (evaluated at s_c) of random variable I_{cc}. The detailed derivation of (7) will be elaborated on in Appendix A.

To reduce the large-scale path loss on the wireless links, we assume that each ACU always prefers to access its nearest BS for maximizing the received power at the latter. Following PPP model [28], the probability density function (PDF) of a randomly chosen CL can be given by $f(r_c) = e^{-\lambda_c \pi r_c^2}(2\pi\lambda_c r_c)$.

The Laplace transform of random variable I_{cc} in (7) can be formulated by

$$\mathcal{L}\left(s_c I_{cc}\right) = \exp\left[-2\pi\lambda_c r_c^2 \rho(\alpha,\epsilon)\right] \tag{8}$$

where $\rho(\alpha,\epsilon) = \frac{\epsilon}{(1-\frac{2}{\alpha})^2}({}_2F_1)(1, 1-\frac{2}{\alpha}; 2-\frac{2}{\alpha}; -\epsilon)$, in which $({}_pF_q)(\cdot)$ denotes the generalized hypergeometric function, as defined in [36]:

$$\begin{aligned}&({}_pF_q)\left(\Theta_1, \Theta_2, \ldots, \Theta_p; \beta_1, \beta_2, \ldots, \beta_q; z\right)\\ &= \sum_{k=0}^{\infty} \frac{(\Theta_1)_k (\Theta_2)_k \cdots (\Theta_p)_k}{(\beta_1)_k (\beta_2)_k \cdots (\beta_q)_k} \frac{z^k}{k!}\end{aligned} \tag{9}$$

The detailed derivation of (8) is elaborated on in Appendix B. By substituting (8) into (7) and setting the negligible thermal noise power to zero,[5] the closed-form of CLs' STP can be derived:

$$\mathcal{S}_c^{(\mathrm{ND})} = \frac{1 - e^{-\lambda_c \pi R^2 [1+2\rho(\alpha,\epsilon)]}}{1 + 2\rho(\alpha,\epsilon)} \tag{10}$$

2) DLs Are Activated Alone: By mitigating the CUs' activation during their co-spectrum ADUs' activating time, the interference contributed by only DLs should be considered in expressing the SINR. In this case, the STP expressions for DLs in both FD and HD modes can be formulated:

$$\begin{cases} \mathcal{S}_d^{(\mathrm{FC})} = \mathcal{L}\left(s_d I_{dd}^{(\mathrm{FD})}\right) e^{-s_d(\sigma^2 + I_{\mathrm{RSI}})} \\ \mathcal{S}_d^{(\mathrm{HC})} = \mathcal{L}\left(s_d I_{dd}^{(\mathrm{HD})}\right) e^{-s_d \sigma^2} \end{cases} \tag{11}$$

where $s_d = \epsilon R_d^{\alpha}/\mathcal{P}_d$. Similarly, (11) has been derived relying on (7). Furthermore, $\mathcal{L}(s_d I_{dd}^{(\mathrm{FD})})$ and $\mathcal{L}(s_d I_{dd}^{(\mathrm{HD})})$ denote the Laplace transform (evaluated at s_d) of random variables $I_{dd}^{(\mathrm{FD})}$ and $I_{dd}^{(\mathrm{HD})}$, respectively, as given by

$$\begin{cases} \mathcal{L}\left(s_d I_{dd}^{(\mathrm{FD})}\right) = \exp\left[-2\pi\lambda_d \int_0^{\infty} g(s_d, x, R_d, \varphi) x dx\right] \\ \mathcal{L}\left(s_d I_{dd}^{(\mathrm{HD})}\right) = \exp\left[-\pi\lambda_d R_d^2 \delta(\alpha,\epsilon)\right] \end{cases} \tag{12}$$

where $\delta(\alpha,\epsilon) = \frac{2\pi\epsilon^{2/\alpha}}{\alpha \sin(2\pi/\alpha)}$ and $g(s,x,r_d,\varphi) = 1 - \frac{1}{1+s\mathcal{P}_d x^{-\alpha}} \frac{1}{1+s\mathcal{P}_d \|x + R_d(\cos\varphi_i, \sin\varphi_i))\|^{-\alpha}}$. Similar to $\mathcal{L}(s_c I_{cc})$, the Laplace transforms of $I_{dd}^{(\mathrm{HD})}$ can also be calculated. The detailed derivation of $\mathcal{L}(s_d I_{dd}^{(\mathrm{FD})})$ is given by Appendix C.

By combining $\mathcal{L}(s_d I_{dd}^{(\mathrm{HD})})$ and $\mathcal{S}_d^{(\mathrm{HC})}$ while setting the thermal noise power to zero, the closed-form of HD mode DLs' STP can be derived:

$$\mathcal{S}_d^{(\mathrm{HC})} = \exp\left[-\pi\lambda_d R_d^2 \delta(\alpha,\epsilon)\right] \tag{13}$$

[5]When the received power is high enough, the impact of the noise power on STP can be neglected.

Since $g(s_d, x, R_d, \varphi)$ in $\mathcal{L}(s_d I_{dd}^{(\mathrm{FD})})$ is hard to deal with by using elementary analytic method, if not impossible, the tight bounds instead of the closed-form of $\mathcal{L}(s_d I_{dd}^{(\mathrm{FD})})$ can be employed for evaluating this Laplace transform.

By using $\overline{\tau}$ and $\underline{\tau}$ to represent the upper and lower bounds of τ, respectively, the tight bounds of $\mathcal{L}(s_d I_{dd}^{(\mathrm{FD})})$ can be expressed:

$$\begin{cases} \overline{\mathcal{L}}\left(s_d I_{dd}^{(\mathrm{FD})}\right) = \exp\left[-(1+\frac{2}{\alpha})\pi\lambda_d R_d^2 \delta(\alpha,\epsilon)\right] \\ \underline{\mathcal{L}}\left(s_d I_{dd}^{(\mathrm{FD})}\right) = \exp\left[-2\pi\lambda_d R_d^2 \delta(\alpha,\epsilon)\right] \end{cases} \tag{14}$$

The Proof of (14) is given by Appendix D. By substituting (14) into $\mathcal{S}_d^{(\mathrm{FC})}$, the tight bounds of FD mode DLs' STP can be expressed:

$$\begin{cases} \overline{\mathcal{S}}_d^{(\mathrm{FC})} = \exp\left[-(1+\frac{2}{\alpha})\pi\lambda_d R_d^2 \delta(\alpha,\epsilon) - \epsilon R_d^{\alpha}/\mu\right] \\ \underline{\mathcal{S}}_d^{(\mathrm{FC})} = \exp\left[-2\pi\lambda_d R_d^2 \delta(\alpha,\epsilon) - \epsilon R_d^{\alpha}/\mu\right] \end{cases} \tag{15}$$

B. CLs and Co-Spectrum DLs Are Allowed to be Activated Simultaneously

1) CLs in Both FD and HD Modes: In this case, the CLs' STP under either FD or HD mode can be formulated by

$$\begin{cases} \mathcal{S}_c^{(\mathrm{FD})} = \int_0^R \left[\mathcal{L}\left(s_c I_{dc}^{(\mathrm{FD})}\right) \mathcal{L}\left(s_c I_{cc}\right) e^{-s_c \sigma^2} f(r_c)\right] dr_c \\ \mathcal{S}_c^{(\mathrm{HD})} = \int_0^R \left[\mathcal{L}\left(s_c I_{dc}^{(\mathrm{HD})}\right) \mathcal{L}\left(s_c I_{cc}\right) e^{-s_c \sigma^2} f(r_c)\right] dr_c \end{cases} \tag{16}$$

where $\mathcal{L}(s_c I_{dc}^{(\mathrm{FD})})$ and $\mathcal{L}(s_c I_{dc}^{(\mathrm{HD})})$ denote the Laplace transform (evaluated at s_c) of random variable $I_{dc}^{(\mathrm{FD})}$ and $I_{dc}^{(\mathrm{HD})}$, respectively, as given by

$$\begin{cases} \mathcal{L}\left(s_c I_{dc}^{(\mathrm{FD})}\right) = \exp\left[-2\pi\lambda_d \int_0^{\infty} g(s_c, x, R_d, \varphi) x dx\right] \\ \mathcal{L}\left(s_c I_{dc}^{(\mathrm{HD})}\right) = \exp\left[-\pi\lambda_d r_c^2 (\frac{\mathcal{P}_d}{\mathcal{P}_c})^{\frac{2}{\alpha}} \delta(\alpha,\epsilon)\right] \end{cases} \tag{17}$$

Similar to $\mathcal{L}(s_d I_{dd}^{(\mathrm{FD})})$, $\mathcal{L}(s_c I_{dc}^{(\mathrm{FD})})$ can also be derived, as shown in Appendix B. Furthermore, similar to $\mathcal{L}(s_c I_{cc})$, we can also derive $\mathcal{L}(s_c I_{dc}^{(\mathrm{FD})})$, as elaborated on in Appendix A.

By combining $\mathcal{L}(s_c I_{dc}^{(\mathrm{HD})})$ and $\mathcal{S}_c^{(\mathrm{HC})}$ while setting the thermal noise power to zero, the closed-form of HD mode CLs' STP can be expressed

$$\mathcal{S}_c^{(\mathrm{HD})} = \frac{1 - e^{-\lambda_c \pi R^2 [1 + \frac{\lambda_d}{\lambda_c}\left(\frac{\mathcal{P}_d}{\mathcal{P}_c}\right)^{\frac{2}{\alpha}} \delta(\alpha,\epsilon) + 2\rho(\alpha,\epsilon)]}}{1 + \frac{\lambda_d}{\lambda_c}\left(\frac{\mathcal{P}_d}{\mathcal{P}_c}\right)^{\frac{2}{\alpha}} \delta(\alpha,\epsilon) + 2\rho(\alpha,\epsilon)}, \tag{18}$$

Similar to $\mathcal{L}(s_d I_{dd}^{(\mathrm{FD})})$, the tight bounds of $\mathcal{L}(s_c I_{dc}^{(\mathrm{FD})})$ can be given by

$$\begin{cases} \overline{\mathcal{L}}\left(s_c I_{dc}^{(\mathrm{FD})}\right) = \exp\left[-\left(1+\frac{2}{\alpha}\right)\pi\lambda_d r_c^2 \left(\frac{\mathcal{P}_d}{\mathcal{P}_c}\right)^{\frac{2}{\alpha}} \delta(\alpha,\epsilon)\right] \\ \underline{\mathcal{L}}\left(s_c I_{dc}^{(\mathrm{FD})}\right) = \exp\left[-2\pi\lambda_d r_c^2 \left(\frac{\mathcal{P}_d}{\mathcal{P}_c}\right)^{2/\alpha} \delta(\alpha,\epsilon)\right] \end{cases} \tag{19}$$

By substituting (19) into $\mathcal{S}_c^{(\mathrm{FD})}$ while setting the thermal noise power to zero, the tight bounds of the CLs' STP in FD mode can

be expressed:

$$\begin{cases} \overline{\mathcal{S}}_c^{(\mathrm{FD})} = \dfrac{1-e^{-\lambda_c\pi R^2[1+(1+\frac{2}{\alpha})\frac{\lambda_d}{\lambda_c}(\frac{\mathcal{P}_d}{\mathcal{P}_c})^{\frac{2}{\alpha}}\delta(\alpha,\epsilon)+2\rho(\alpha,\epsilon)]}}{1+(1+\frac{2}{\alpha})\frac{\lambda_d}{\lambda_c}(\frac{\mathcal{P}_d}{\mathcal{P}_c})^{\frac{2}{\alpha}}\delta(\alpha,\epsilon)+2\rho(\alpha,\epsilon)} \\ \underline{\mathcal{S}}_c^{(\mathrm{FD})} = \dfrac{1-e^{-\lambda_c\pi R^2[1+2\frac{\lambda_d}{\lambda_c}(\frac{\mathcal{P}_d}{\mathcal{P}_c})^{\frac{2}{\alpha}}\delta(\alpha,\epsilon)+2\rho(\alpha,\epsilon)]}}{1+2\frac{\lambda_d}{\lambda_c}(\frac{\mathcal{P}_d}{\mathcal{P}_c})^{\frac{2}{\alpha}}\delta(\alpha,\epsilon)+2\rho(\alpha,\epsilon)} \end{cases} \tag{20}$$

2) DLs in Both FD and HD Modes: In this case, the FD DLs' STP ($\mathcal{S}_d^{(\mathrm{FD})}$) and HD DLs' STP ($\mathcal{S}_d^{(\mathrm{HD})}$) can be expressed:

$$\begin{cases} \mathcal{S}_d^{(\mathrm{FD})} = \mathcal{L}\left(s_d I_{dd}^{(\mathrm{FD})}\right)\mathcal{L}\left(s_d I_{cd}\right)e^{-s_d(\sigma^2+I_{\mathrm{RSI}})} \\ \mathcal{S}_d^{(\mathrm{HD})} = \mathcal{L}\left(s_d I_{dd}^{(\mathrm{HD})}\right)\mathcal{L}\left(s_d I_{cd}\right)e^{-s_d\sigma^2} \end{cases} \tag{21}$$

where $s_d = \epsilon R_d^\alpha/\mathcal{P}_d$. Similar to $\mathcal{L}(s_c I_{cc})$, the Laplace transform (evaluated at s_d) of random variable I_{cd} can be calculated:

$$\mathcal{L}\left(s_d I_{cd}\right) = \exp\left[-\pi\lambda_c R_d^2\left(\frac{\mathcal{P}_c}{\mathcal{P}_d}\right)^{\frac{2}{\alpha}}\delta(\alpha,\epsilon)\right] \tag{22}$$

By substituting both $\mathcal{L}(s_d I_{dd}^{(\mathrm{HD})})$ in (12) and $\mathcal{L}(s_d I_{cd})$ in (22) into $\mathcal{S}_d^{(\mathrm{HD})}$, while setting the thermal noise power to zero, the closed-form of HD mode DLs' STP can be derived:

$$\mathcal{S}_d^{(\mathrm{HD})} = \exp\left[-\pi\lambda_c R_d^2\left(\frac{\mathcal{P}_c}{\mathcal{P}_d}\right)^{\frac{2}{\alpha}}\delta(\alpha,\epsilon) - \pi\lambda_d R_d^2\delta(\alpha,\epsilon)\right] \tag{23}$$

By substituting both (14) and (22) into $\mathcal{S}_d^{(\mathrm{FD})}$ while setting the thermal noise power to zero, the tight bounds of FD mode DLs' STP can be attained:

$$\begin{cases} \overline{\mathcal{S}}_d^{(\mathrm{FD})} = \exp\left[-\pi\lambda_c R_d^2\left(\frac{\mathcal{P}_c}{\mathcal{P}_d}\right)^{\frac{2}{\alpha}}\delta(\alpha,\epsilon) - \epsilon R_d^\alpha/\mu\right] \\ \qquad\qquad \cdot\exp\left[-\left(1+\frac{2}{\alpha}\right)\pi\lambda_d R_d^2\delta(\alpha,\epsilon)\right] \\ \underline{\mathcal{S}}_d^{(\mathrm{FD})} = \exp\left[-\pi\lambda_c R_d^2\left(\frac{\mathcal{P}_c}{\mathcal{P}_d}\right)^{\frac{2}{\alpha}}\delta(\alpha,\epsilon) - \epsilon R_d^\alpha/\mu\right] \\ \qquad\qquad \cdot\exp\left[-2\pi\lambda_d R_d^2\delta(\alpha,\epsilon)\right] \end{cases} \tag{24}$$

V. The Average Coverage Probability for Both CLs and DLs

Relying on STP, which determines whether a single user's data transmission is successful or not, the performance of the whole underlaying CN can be evaluated. To study the statistical characteristics of all users, we may employ the ACP of both CLs and DLs for evaluating the quality of a randomly chosen CL/DL that reaches its predetermined SINR target. The ACP can be calculated by using $\mathbb{E}(S) = \mathbb{P}_{\mathrm{OP}}\cdot S$, where $\mathbb{P}_{\mathrm{OP}}$ and S denote the OP and STP of the chosen CU/DU, respectively.

Let us consider the following three scenarios, as illustrated in Fig. 2:

- **Scenario I**: a time slot is exclusively occupied by ACUs;
- **Scenario II**: a time slot is exclusively occupied by ADUs;
- **Scenario III**: a time slot is shared by both ACUs and co-spectrum ADUs.

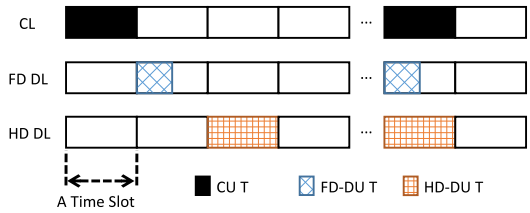

Fig. 2. The scenarios corresponding to the time slot occupied by CL, FD DL and HD-DL, respectively, where we use "CU T," "FD-DU T" and "HD-DU T" to specify the transmitting phases of CU, FD-DU and HD-DU, respectively.

Unlike the first two scenarios, if CUs and their co-spectrum DUs are allowed to keep activation simultaneously, things will change: FD-ADUs can spend half the time of HD-ADUs to achieve the same amount of data exchange as the latter. Although ADUs (either FD-ADUs or HD-ADUs) will always impose an interfere on their co-spectrum ACUs whenever they are both activated, FD-ADUs can always save half the time slot to create a non-interfering[6] environment for ACUs. In contrast, HD-ADUs will continue to impose interference on ACUs throughout the time slot.

To better analyze the performance gain of FD-ADUs brought about by "compressing activation time to half of HD-ADUs," we may employ OP for evaluating CLs/DLs' STPs. In the following, we assume that $N = N_c + N_d$ users are allowed to share the same spectrum, where N_c and N_d denote the number of ACUs and ADUs, respectively. Following the PPP model, the expected number of ACUs and ADUs inside a radius-R cell can be expressed by $\mathbb{E}(N_c) = \lambda_c\pi R^2$ and $\mathbb{E}(N_d) = \lambda_d\pi R^2$, respectively. Furthermore, relying on the definition of OP, the probabilities that the CUs (or DUs) are not occupying a given time slot can be calculated:

$$\begin{cases} \check{\mathbb{P}}_c = (1-\mathbb{P}_c)^{N_c} \\ \check{\mathbb{P}}_f = (1-\mathbb{P}_f)^{N_d} \\ \check{\mathbb{P}}_h = (1-\mathbb{P}_h)^{N_d} \end{cases} \tag{25}$$

Following the above-mentioned analysis, we can give out the probabilities that the CUs, FD-DUs and HD-DUs keep activation within a given time slot as $\hat{\mathbb{P}}_c = 1-\check{\mathbb{P}}_c$, $\hat{\mathbb{P}}_f = 1-\check{\mathbb{P}}_f$ and $\hat{\mathbb{P}}_h = 1-\check{\mathbb{P}}_h$, respectively. In particular, by considering FNs, the ACPs for CLs/DLs can be expressed:

$$\begin{cases} \mathcal{S}_c^f = \hat{\mathbb{P}}_f\cdot\left[\mathcal{S}_c^{(\mathrm{FD})}\right]^{N_c} + \check{\mathbb{P}}_f\cdot\left[\mathcal{S}_c^{(\mathrm{ND})}\right]^{N_c} \\ \mathcal{S}_d^f = \hat{\mathbb{P}}_c\cdot\left[\mathcal{S}_d^{(\mathrm{FD})}\right]^{N_d} + \check{\mathbb{P}}_f\cdot\left[\mathcal{S}_d^{(\mathrm{FC})}\right]^{N_d} \end{cases} \tag{26}$$

Similarly, by considering HNs, we can also give out the ACPs for CLs/DLs:

$$\begin{cases} \mathcal{S}_c^h = \hat{\mathbb{P}}_h\cdot\left[\mathcal{S}_c^{(\mathrm{HD})}\right]^{N_c} + \check{\mathbb{P}}_h\cdot\left[\mathcal{S}_c^{(\mathrm{ND})}\right]^{N_c} \\ \mathcal{S}_d^h = \hat{\mathbb{P}}_c\cdot\left[\mathcal{S}_d^{(\mathrm{HD})}\right]^{N_d} + \check{\mathbb{P}}_c\cdot\left[\mathcal{S}_d^{(HC)}\right]^{N_d} \end{cases} \tag{27}$$

[6]We mean the "D2D-induced" interference.

VI. Sum Throughput and Its Break Point for D2D-Aided Underlaying CNs

One of the purposes for enabling D2D in CNs is to improve the sum throughput of the whole network. It should be emphasized that while D2D technology brings increased network throughput, the activating DUs will always cause certain interference to close-range co-spectrum CUs. In this subsection, we will evaluate the sum throughput of both FNs and HNs. To analyze the impact of workload density on sum throughput, the maximum sum throughput of both FNs and HNs parameterized by OP will be evaluated. Relying on the above analysis, we can select the optimal mode by comparing the performance of FNs and HNs.

A. Sum Throughput for Both FNs and HNs

1) Nearly Closed-Form of ACPs in FNs: To derive the sum throughput of FNs/HNs, we may employ the nearly closed-form expressions of S_c^f and S_d^f that was given by (26). Let us define $\mathbb{P}_c = \eta\mathbb{P}_f$, where η is a given constant that determines $\eta_1 = \lambda_d/\lambda_c = (\bar{\lambda_d}\mathbb{P}_{ad})/(\bar{\lambda_c}\mathbb{P}_{ac}) = (2\bar{\lambda_d}\mathbb{P}_f)/(\bar{\lambda_c}\mathbb{P}_c) = (2/\eta)(\bar{\lambda_d}/\bar{\lambda_c})$, which is also a constant. By observing the tight bounds of $\mathcal{S}_d^{(\mathrm{FC})}$, $\mathcal{S}_c^{(\mathrm{FD})}$ and $\mathcal{S}_d^{(\mathrm{FD})}$ that were defined in (15), (20) and (24), respectively, we need to define two additional constants, i.e., ς_1 and ς_2, whose values are both in $[1+2/\alpha, 2]$.

Following the above-mentioned definitions, the nearly closed-form expressions of $\mathcal{S}_d^{(\mathrm{FC})}$, $\mathcal{S}_c^{(\mathrm{FD})}$ and $\mathcal{S}_d^{(\mathrm{FD})}$ can be derived:

$$\begin{cases} \mathcal{S}_d^{(\mathrm{FC})} = \exp\left[-2\bar{\lambda_d}\varsigma_2\pi R_d^2\delta(\alpha,\epsilon)\mathbb{P}_f - \epsilon R_d^\alpha/\mu\right] \\ \mathcal{S}_c^{(\mathrm{FD})} \approx \dfrac{1-e^{-\bar{\lambda_c}\eta\pi R^2\mathbb{P}_f}}{1+\varsigma_1\eta_1 P\delta(\alpha,\epsilon)+2\rho(\alpha,\epsilon)} \\ \mathcal{S}_d^{(\mathrm{FD})} = \exp\left[-2\bar{\lambda_d}(\eta_1 P)^{-1}\delta(\alpha,\epsilon)\pi R_d^2\mathbb{P}_f - \epsilon R_d^\alpha/\mu\right] \\ \qquad\qquad \cdot \exp\left[-2\bar{\lambda_d}\varsigma_2\pi R_d^2\delta(\alpha,\epsilon)\mathbb{P}_f\right] \end{cases} \tag{28}$$

where $P = (\mathcal{P}_d/\mathcal{P}_c)^{2/\alpha}$. Furthermore, $\mathcal{S}_c^{(\mathrm{ND})}$ can be expressed:

$$\mathcal{S}_c^{(\mathrm{ND})} \approx \frac{1-e^{-\bar{\lambda_c}\eta\pi R^2\mathbb{P}_f}}{1+2\rho(\alpha,\epsilon)} \tag{29}$$

By employing the Taylor expansion of e^z with Peyano Remainder $e^z = 1+\frac{1}{1!}z+\frac{1}{2!}z^2+\frac{1}{3!}z^3+O(z^3)$, we may approximate $\mathcal{S}_c^{(\mathrm{FD})}$, $\mathcal{S}_d^{(\mathrm{FD})}$, $\mathcal{S}_d^{(\mathrm{FC})}$ and $\mathcal{S}_c^{(\mathrm{ND})}$, respectively, as (by taking the first two items in each expansion):

$$\begin{cases} \mathcal{S}_c^{(\mathrm{FD})} \approx \varpi_1\kappa_1\mathbb{P}_f \\ \mathcal{S}_d^{(\mathrm{FD})} \approx \varpi_3\left[1-(\kappa_2+\kappa_3)\,\mathbb{P}_f\right] \\ \mathcal{S}_d^{(\mathrm{FC})} \approx \varpi_3\left(1-\kappa_3\mathbb{P}_f\right) \\ \mathcal{S}_c^{(\mathrm{ND})} \approx \varpi_2\kappa_1\mathbb{P}_f \end{cases} \tag{30}$$

where $\varpi_1 = 1/[1+\varsigma_1\eta_1 P\delta(\alpha,\epsilon)+2\rho(\alpha,\epsilon)]$, $\varpi_2 = 1/[1+2\rho(\alpha,\epsilon)]$ and $\varpi_3 = \exp[-\epsilon R_d^\alpha/\mu]$, $\kappa_1 = \bar{\lambda_c}\eta\pi R^2$, $\kappa_2 = 2\bar{\lambda_d}(\eta_1 P)^{-1}\delta(\alpha,\epsilon)\pi R_d^2$ and $\kappa_3 = 2\bar{\lambda_d}\varsigma_2\pi R_d^2\delta(\alpha,\epsilon)$.

By substituting (30) into (26) and tidying them up, the nearly closed-form of ACPs for CLs/DLs in FNs can be expressed:

$$\begin{cases} \tilde{\mathcal{S}_c^f} \approx \kappa_1^{N_c}\left[\varpi_1^{N_c}+\left(\varpi_2^{N_c}-\varpi_1^{N_c}\right)(1-\mathbb{P}_f)^{N_d}\right]\cdot\mathbb{P}_f^{N_c} \\ \tilde{\mathcal{S}_d^f} \approx \varpi_3^{N_d}\left[1-(\kappa_2+\kappa_3)\mathbb{P}_f\right]^{N_d} - \varpi_3^{N_d}\left[1-\eta\mathbb{P}_f\right]^{N_c} \\ \qquad\qquad \cdot\left\{\left[1-(\kappa_2+\kappa_3)\mathbb{P}_f\right]^{N_d} - \left[1-\kappa_3\mathbb{P}_f\right]^{N_d}\right\} \end{cases} \tag{31}$$

2) Nearly Closed-Form of ACPs in HNs: The closed-form of $\mathcal{S}_c^{(\mathrm{HD})}$, $\mathcal{S}_d^{(\mathrm{HD})}$ and $\mathcal{S}_d^{(\mathrm{HC})}$ can be given by:

$$\begin{cases} \mathcal{S}_c^{(\mathrm{HD})} \approx \dfrac{1-e^{-\bar{\lambda_c}\eta\pi R^2\mathbb{P}_f}}{1+\eta_1 P\delta(\alpha,\epsilon)+2\rho(\alpha,\epsilon)} \\ \mathcal{S}_d^{(\mathrm{HD})} = \exp\left[-2\bar{\lambda_d}(\eta_1 P)^{-1}\delta(\alpha,\epsilon)\pi R_d^2\mathbb{P}_f\right] \\ \qquad\qquad \cdot\exp\left[-2\bar{\lambda_d}\pi R_d^2\delta(\alpha,\epsilon)\mathbb{P}_f\right] \\ \mathcal{S}_d^{(\mathrm{HC})} = \exp\left[-2\bar{\lambda_d}\pi R_d^2\delta(\alpha,\epsilon)\mathbb{P}_f\right] \end{cases} \tag{32}$$

By keeping the first two items of the Taylor expansion of each expression, the nearly closed-form of $\mathcal{S}_c^{(\mathrm{HD})}$, $\mathcal{S}_d^{(\mathrm{HD})}$ and $\mathcal{S}_d^{(\mathrm{HC})}$ can be given by:

$$\begin{cases} \mathcal{S}_c^{(\mathrm{HD})} \approx \varpi_4\kappa_1\mathbb{P}_f \\ \mathcal{S}_d^{(\mathrm{HD})} \approx 1-(\kappa_2+\kappa_4)\,\mathbb{P}_f \\ \mathcal{S}_d^{(\mathrm{HC})} \approx 1-\kappa_4\mathbb{P}_f \end{cases} \tag{33}$$

where $\varpi_4 = 1/[1+\eta_1 P\delta(\alpha,\epsilon)+2\rho(\alpha,\epsilon)]$ and $\kappa_4 = 2\bar{\lambda_d}\pi R_d^2\delta(\alpha,\epsilon)$.

By substituting (33) and $\mathcal{S}_c^{(\mathrm{ND})}$ into (27) and tidying them up,[7] the nearly closed-form of ACPs for CLs/DLs in HNs can be expressed:

$$\begin{cases} \tilde{\mathcal{S}_c^h} \approx \kappa_4^{N_c}\left[\varpi_1^{N_c}+\left(\varpi_2^{N_c}-\varpi_4^{N_c}\right)(1-\mathbb{P}_f)^{N_d}\right]\cdot\mathbb{P}_f^{N_c} \\ \tilde{\mathcal{S}_d^h} \approx \left[1-(\kappa_2+\kappa_4)\mathbb{P}_f\right]^{N_d} - \left[1-\eta\mathbb{P}_f\right]^{N_c} \\ \qquad\qquad \cdot\left\{\left[1-(\kappa_2+\kappa_4)\mathbb{P}_f\right]^{N_d} - \left[1-\kappa_4\mathbb{P}_f\right]^{N_d}\right\} \end{cases} \tag{34}$$

3) Sum Throughput of FNs and HNs: By defining the sum throughput of a D2D-aided underlaying CN as $\mathcal{T} = \lambda\mathcal{S}\log(1+\epsilon)$, where λ denotes the node density, $\mathcal{S}$ represents the STP of a typical link and ϵ stands for the SINR, the sum throughput of FNs/HNs can respectively be expressed:

$$\begin{aligned} \mathcal{T}_f &= (\lambda_c\mathcal{S}_c^f + 2\lambda_d\mathcal{S}_d^f)\log(1+\epsilon) \\ &\approx \varpi_5\mathbb{P}_f\tilde{\mathcal{S}_c^f} + \varpi_6\mathbb{P}_f\tilde{\mathcal{S}_d^f} \end{aligned} \tag{35}$$

and

$$\begin{aligned} \mathcal{T}_h &= (\lambda_c\mathcal{S}_c^h + \lambda_d\mathcal{S}_d^h)\log(1+\epsilon) \\ &\approx \varpi_5\mathbb{P}_f\tilde{\mathcal{S}_c^h} + \varpi_6\mathbb{P}_f\tilde{\mathcal{S}_d^h} \end{aligned} \tag{36}$$

where $\varpi_5 = 2\bar{\lambda_d}\eta_1^{-1}\log(1+\epsilon)$ and $\varpi_6 = 4\bar{\lambda_d}\log(1+\epsilon)$.

[7]Please refer to (29) for the expression of $\mathcal{S}_c^{(ND)}$. Note that $\mathcal{S}_c^{(\mathrm{ND})}$ has the same definition and expression in both FNs and HNs.

B. Maximum Sum Throughput of FNs/HNs

Note that an increased OP implies a severer interference that imposed on the existing ACUs/ADUs due to the increased AU densities, if the spectrum allocation among users is not perfectly orthogonal (i.e., there exists non-zero inter-user interference). In this case, the sum throughput of D2D-aided underlaying CNs cannot be unlimitedly improved by simply (infinitely) increasing the OP.

By investigating the impact of (including $\mathbb{P}_c$, $\mathbb{P}_h$ and $\mathbb{P}_f$) on sum throughput of the underlaying CNs, we should derive the expression of the maximum sum throughput (MST) for both FNs and HNs. Let us first give out the following assumptions:

- the cellular radius is kept fixed;
- the average distance between D2D pairs is a constant;
- a constant transmit power, i.e., $\mathcal{P}_c$ and $\mathcal{P}_d$ for CUs and DUs, respectively, is considered;
- a steady user density, i.e., $\bar{\lambda_c}$ and $\bar{\lambda_d}$ for CUs and DUs, respectively, is considered.

Following the above assumptions, the sum throughput of FNs will be overwhelmingly determined by the factor $\mathbb{P}_f$. In order to derive the MST of FNs/HNs, let us take partial derivative to $\mathcal{T}_f$ and $\mathcal{T}_h$ with respect to $\mathbb{P}_f$:

$$\begin{cases} \dfrac{\partial \mathcal{T}_f}{\partial \mathbb{P}_f} \approx \varpi_5 \tilde{\mathcal{S}_c^f} + \varpi_6 \tilde{\mathcal{S}_d^f} + \mathbb{P}_f \left(\varpi_5 \dfrac{\partial \tilde{\mathcal{S}_c^f}}{\partial \mathbb{P}_f} + \varpi_6 \dfrac{\partial \tilde{\mathcal{S}_d^f}}{\partial \mathbb{P}_f} \right) \\ \dfrac{\partial \mathcal{T}_h}{\partial \mathbb{P}_f} \approx \varpi_5 \tilde{\mathcal{S}_c^h} + \varpi_6 \tilde{\mathcal{S}_d^h} + \mathbb{P}_f \left(\varpi_5 \dfrac{\partial \tilde{\mathcal{S}_c^h}}{\partial \mathbb{P}_f} + \varpi_6 \dfrac{\partial \tilde{\mathcal{S}_d^h}}{\partial \mathbb{P}_f} \right) \end{cases} \tag{37}$$

By setting $\frac{\partial \mathcal{T}_f}{\partial \mathbb{P}_f} = 0$ and $\frac{\partial \mathcal{T}_h}{\partial \mathbb{P}_f} = 0$, we get a complicated one-element-of-high-order equation, whose solutions correspond to the maximum sum throughput. Since both equations are continuous functions, Newton-Raphson method can be employed for solving them. The optimal OP (i.e., $\mathbb{P}_{opt}^f$ or $\mathbb{P}_{opt}^h$) that leads to the MST of FNs/HNs can thus be identified.

The detailed equation-solving process is illustrated in Table II, in which we used $\partial \mathcal{T}_f / \partial \mathbb{P}_f = 0$ as an example to show the solution process of this equation. In fact, the solution process of the above equation can be understood as an extreme point search process relying on Newton-Raphson method in terms of $\mathbb{P}_f$. Both the optimal OP and MST of FNs/HNs can be derived by employing the above-mentioned method.

TABLE II
EQUATION-SOLVING PROCESS RELYING ON NEWTON-RAPHSON METHOD

Input
Give an initial approximation: $\mathbb{P}_n \in (0, 1/\eta]$
Initialization
Define cost function: $f(\mathbb{P}_f) = \dfrac{\partial \mathcal{T}_f}{\partial \mathbb{P}_f}$
Take partial derivative to this cost function: $f'(\mathbb{P}_f) = \dfrac{\partial^2 \mathcal{T}_f}{\partial \mathbb{P}_f^2}$
Set a small-enough error-threshold: $\gamma > 0$
Set solution number: $N_s = 0$
Step#1
Derive a better approximation: $\mathbb{P}_{n+1} = \mathbb{P}_n - \dfrac{f(\mathbb{P}_n)}{f'(\mathbb{P}_n)}$
if $\mathbb{P}_{n+1} < 0$ or $\mathbb{P}_{n+1} > 1/\eta$
go to Step #3
else
go to Step #2
Step#2
if $\mid f(\mathbb{P}_{n+1}) \mid \leq \gamma$
$N_s = N_s + 1$
$\mathbb{P}_{N_s} = \mathbb{P}_{n+1}$;
set $\mathbb{P}_n = \mathbb{P}_{n+1} + \gamma$;
if $\mathbb{P}_n < 0$ or $\mathbb{P}_n > 1/\eta$
go to Step #3
else
go to Step #1
else
set $\mathbb{P}_n = \mathbb{P}_{n+1}$ and go to Step #1
Step#3
$\mathbb{P}_{opt}^f = \max\limits_{\mathbb{P}_{Ns}} \mathcal{T}_f(\vec{\mathbb{P}}_{N_s})$
Output
Output the optimal OP $\mathbb{P}_{opt}^f$ and the MST $\mathcal{T}_f\left(\mathbb{P}_{opt}^f\right)$

C. Optimal D2D Mode Selection

To maximize the sum throughput of the D2D-aided underlaying CNs, the cost function (i.e., the optimization problem) can be formulated as:

$$\max_{(\mathbb{P}_f, \eta, \zeta_1, \zeta_2)} \ (\mathcal{T}_f, \mathcal{T}_h)$$
$$\text{s.t.} \quad 0 \leq \mathbb{P}_f \leq \frac{1}{\eta} \tag{38}$$

Note that the upper and lower bounds of ζ_1 and ζ_2 can be given by $(1 + 2/\alpha) \leq \zeta_1, \zeta_2 \leq 2$, and η satisfies $\eta \geq 1$. By taking a fixed value for each parameter, including $\bar{\lambda}_c$, $\bar{\lambda}_d$, P, α, ϵ, μ, ζ_1, ζ_2, η, and $\mathbb{P}_f$), we can compare the values of $\mathcal{T}_f$ and $\mathcal{T}_h$ under a fair condition.

VII. NUMERIC ANALYSIS

In this section, the performance of the proposed D2D-aided underlaying CNs in terms of ACP and sum throughput will be evaluated. Duplex mode selection between FD and HD will then be performed according to the above-mentioned results. By comparing the performance of FNs and HNs, the optimal duplex mode under appropriate configurations can be attained.

In the following, the impact of OP on both ACP and sum throughput will be investigated for reflecting the affordable traffic volume in FNs/HNs. Meanwhile, the influence of a variety of critical parameters, including the RSI, the SINR threshold and the number of AUs, will also be took into account. Furthermore, in light of the fact that the explicit values of both ACP and the sum throughput corresponding to $\mathcal{S}_d^{(\mathrm{FC})}$, $\mathcal{S}_d^{(\mathrm{FD})}$ and $\mathcal{S}_c^{(\mathrm{FD})}$ are hard to derive, the tight bounds instead of analytical results will be employed for approximately evaluating the performance of the proposed systems.

A. Simulation Setup

We choose an environment with area $1000 \times 1000\,\mathrm{m}^2$ for performing simulations, within which BSs, CUs and DUs are distributed according to homogeneous PPP models (with densities of $3 \times 10^{-5}\mathrm{m}^{-2}$, $1 \times 10^{-4}\mathrm{m}^{-2}$ and $3 \times 10^{-4}\mathrm{m}^{-2}$, respectively).

TABLE III
SIMULATION PARAMETERS OF THE PROPOSED ANALYSIS

parameters	value
$\mathcal{P}_c$	24 dBm
$\mathcal{P}_d$	20 dBm
R	100 m
R_d	30 m
λ_b	3×10^{-5} users/m^2
λ_c	1×10^{-4} users/m^2
λ_d	3×10^{-4} users/m^2
α	4
η	2

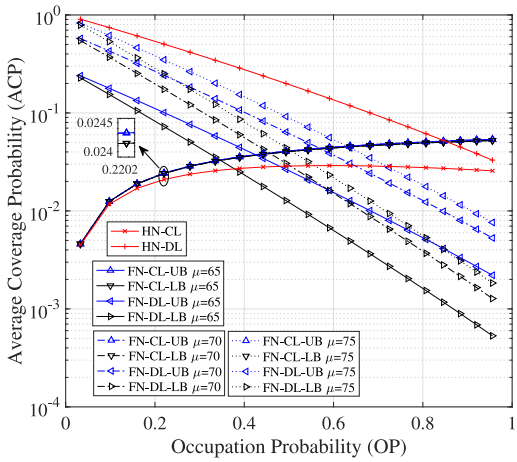

Fig. 3. The ACP-curves for both CL and DL as function of OP with variant μ values when $R_d = 30\,m$ in FNs/HNs, where we use "UB" and "LB" to specify the upper and lower bounds, respectively.

The licensed uplink band that was supposed to be exclusively allocated to CUs is now allowed to be reused by DUs. Without loss of generality, each link is assumed to be an i.i.d. Rayleigh fading channel. Furthermore, the path-loss exponent α is set to be 4 (i.e., corresponding to the typical urban environment). The allowed maximum CU-to-BS distance is supposed to be 100 m, while the average distance between D2D pairs is assumed to be 30 m. In this case, all the CUs within this experimental area are assumed to have the same transmitting power, say 24 dBm, while that of all the DUs are assumed to be 20 dBm. In addition, the APs of CUs and DUs are assumed to be $\mathbb{P}_c$ and $\mathbb{P}_h$, respectively, both of which are constants. Finally, by setting $\eta = 2$, it makes $\mathbb{P}_f = \mathbb{P}_c/2 = \mathbb{P}_h/2$ be satisfied. The parameter settings of the proposed simulations are elaborated on in Table III.

B. Performance Comparison Between FNs and HNs in Terms of OP and RSI

In this subsection, an individual sub-channel is assumed to be reused by one ACU and one ADU. A moderate value of the SINR threshold ϵ, say 5, is chosen. Note that the average RSI power of FD-DUs can be expressed as $I_{\mathrm{RSI}} = \mathcal{P}_d/\mu$, where μ denotes the SIC coefficient. In the following, we will use the SIC coefficient (μ) instead of I_{RSI} to denote the RSI power. As shown in Fig. 3-Fig. 5, the performance of FNs/HNs as a function of both OP and μ can be evaluated and compared.

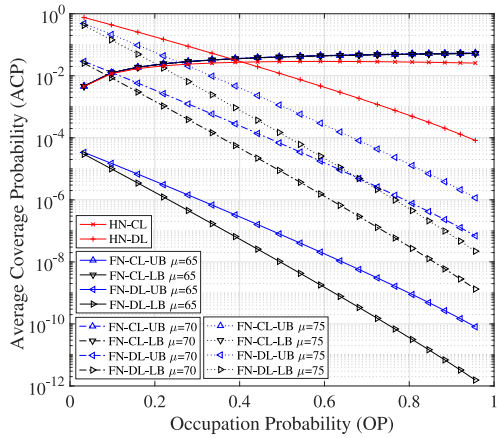

Fig. 4. The ACP-curves for both CL and DL as function of OP with variant μ values when $R_d = 50\,m$ in FNs/HNs, where we use "UB" and "LB" to specify the upper and lower bounds, respectively.

In Fig. 3, the ACP-curves for both CL and DL as function of OP are described, with variant μ in FNs/HNs considered. On the one hand, the ACP of CL in both FNs and HNs (denoted by FN-CL and HN-CL, respectively) are monotonically increasing functions of OP (i.e., slowly raised and converged to a ceiling as OP increases). In particular, the upper bound of CL in the FNs (FN-CL-UB) is shown to have the same trend as the lower bound of DL in the FNs (FN-CL-LB). However, the RSI is shown to have almost no effect on the ACP's upper and lower bounds of FN-CL. We may explain it as follows: the RSI can be understood as a leakage of the transmit signal that was directly coupled into the received signal in an FD-DU, in which the simultaneous transmission and reception occur. In this case, only FD-DLs suffer from the impact of RSI. Furthermore, by comparing (26) with (27), the FN-CL is shown to outperform the HN-CL in terms of ACP due to the smaller OP obtained in the former, although the latter has an advantage on STP. However, in the presence of a severe RSI and a heavier inter-DU-interference, the ACP of DL in the FNs (FN-DL) are shown to be lower than that of DL in the HNs (HN-DL). On the other hand, as OP increases, the ACPs of both FN-DL and HN-DL are shown to reduce rapidly, implying that the DL' ACP is affected by OP more than CL. Furthermore, the RSI is shown to be capable of affecting the ACP of DL, or in other words, a higher value of μ implies a lower value of ACP of DL. Evidently, HN-DL always outperforms HN-CL in terms of ACP, as shown in Fig. 3. We can explain it as follows: Under different statistical configurations of distances, the average distance between D2D pairs in a given cell is assumed to 30 m, while the average CU-to-BS distance is 50 m, where the latter induces a severer path-loss. If the average distance of the D2D pairs is set to be 50 m, the ACP-curves can be re-plotted, as shown in Fig. 4. Compared with Fig. 3, we get higher ACP of CL in Fig. 4. Anyway, as long as OP is high enough (e.g., higher than 0.5), the ACP of CL will always be higher than that of DL.

In Fig. 5, the curves of the sum throughput for both FNs and HNs as functions of OP is illustrated, with the impact of variant μ values considered. The curves of the maximum sum throughput

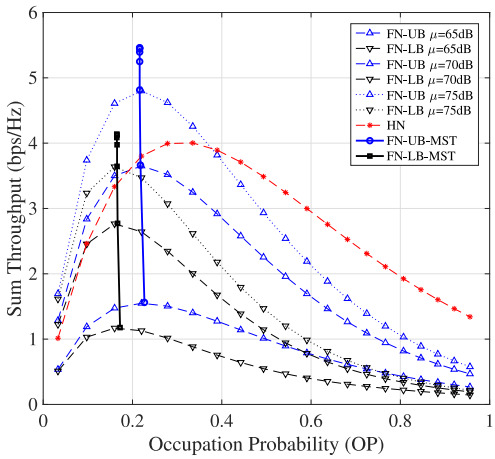

Fig. 5. The sum throughput for both FNs and HNs as a function of OP with variant μ values, where we use "UB" and "LB" to specify the upper and lower bounds, respectively.

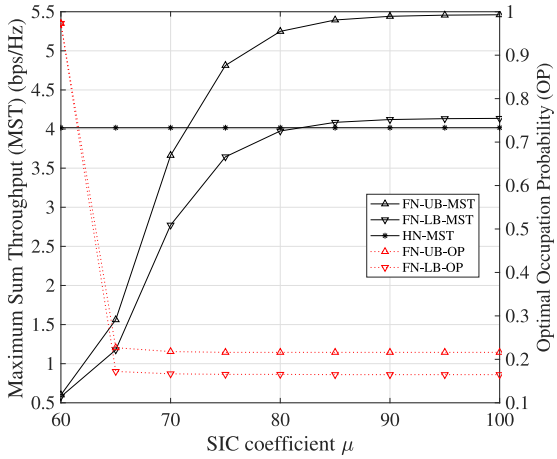

Fig. 6. The curves of the maximum sum throughput as function of OP with variant μ values in both FNs and HNs, where we use "UB" and "LB" to specify the upper and lower bounds, respectively.

(MST) are also plotted by identifying the optimal OP for both the upper and lower bounds of FNs (marked as FN-UB-MST and FN-LB-MST, respectively) corresponding to each μ value. In particular, these two MST curves (from up to down) correspond to μ values from 100 dB to 65 dB. As OP increases from zero, it is shown that the sum throughput of both FNs and HNs increase gradually. Beyond the break points (i.e., correspond to the MST points), the sum throughput will creep down slowly while the OP continually increases. We may explain it as follows: the traffic of both the CUs and DUs are far from saturation when the OP is small, thus making an increasing sum throughput at first. However, the increasing probability of a slot shared by both ACUs and ADUs will then lead to a severer interference that will erode the sum throughput. Therefore, the break points beyond which the sum throughput will creep down must exit. Furthermore, the sum throughput of FNs is greatly affected by the RSI due to the fact that the sum throughput dwindles as μ decreases. Moreover, if focusing on the MST of FNs, the MST of FNs (FN-MST) is shown to be improved as μ increases from 65 dB to 100 dB. However, beyond 80 dB, almost no gain in the MST of the FN can be obtained by further increasing μ. From this perspective, it is meaningless to try to reduce the SI to zero. In addition, there also exits a break-even point between FNs and HNs: when OP is large enough to break this point, HNs will outperform FNs in terms of ACP.

To more effectively optimize the sum throughput, the MST of FNs corresponding to variant μ values are analyzed, as illustrated in Fig. 6. By identifying the optimal OP, the MST of HNs (marked as HN-MST) is also plotted in this figure as a benchmark. It is shown that both the upper and lower bounds of the MST in the FNs are concave functions of μ, i.e., they will increase rapidly as μ increases, and then slowly pace down and tend to be flat. Furthermore, the break-even point is shown to be located at $\mu = 80$ dB, where the MST of FN-LB is higher than that of the HNs (marked as HN in the figure). In addition, the optimal OP values of the tight bounds of FNs (marked as FN-UB-OP and FN-LB-OP, respectively) are shown to be relatively stable along with the MST raising beyond the location of $\mu \geq 65$.

To summarize, as OP increases, the interference growth rate of FNs is about twice the rate of interference growth of HNs, implying that the sum throughput of FNs will be less than that of HNs in the presence of large OPs. Nevertheless, while RSI is small enough (e.g., $\mu \geq 80$ dB), FNs may outperform HNs by employing an appropriately low OP. In contrast, the sum throughput of FNs will be lower than that of HNs in the high-OP scenarios due to the non-neglected interference imposed by DTs.

C. Performance Comparison Between FNs and HNs as a Function of Both OP and SINR Threshold

In this subsection, we assume that an individual sub-channel is shared by one ACU and one ADU. The SIC coefficient μ in FD mode is set to be 75 dB.[8] The performance of FNs/HNs as a function of both OP and SINR threshold (ϵ) will be analyzed in Fig. 7-Fig. 9.

In Fig. 7, the ACP-curves for both CL and DL as functions of OP with variant ϵ values in FNs/HNs are illustrated. As shown in this figure, the DLs will contribute more to the whole networks if OP is small, while CLs will dominate the performance if OP is large. Furthermore, as OP increases, the ACP of the CLs in FNs/HNs is shown to increase and tend to be gentler, while that of DLs is shown to linearly decrease, implying that the break-even points of the sum throughput, which can be derived based on the ACP of both CL and DL, exist in both FNs and HNs. Moreover, the ACP of both CL and DL are shown to suffer from an erosion as ϵ increases. Nevertheless, DL's ACP experiences faster decrease than CL's. In particular, the ACP values with higher SINR threshold are shown to decline with a higher speed. In addition, the ACP of CLs outperforms that of DLs in FNs,

[8]Actually, this is not a demanding and difficult goal, please refer to [19] for details.

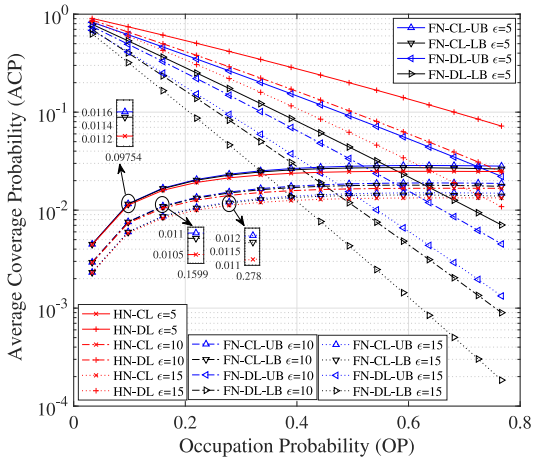

Fig. 7. The ACP-curves for both CL and DL as functions of OP with variant ϵ values in FNs/HNs, where we use "UB" and "LB" to specify the upper and lower bounds, respectively.

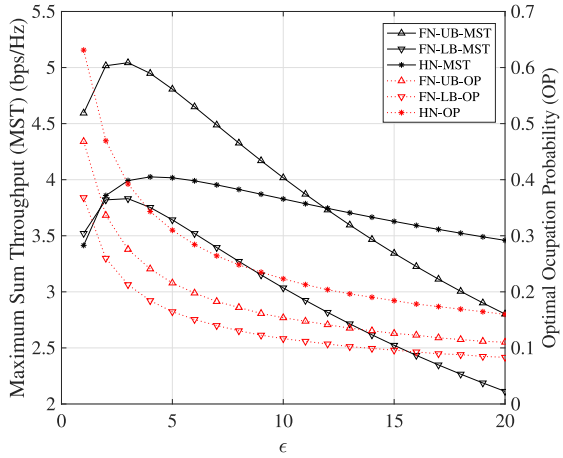

Fig. 9. The curves of the MST in terms of the optimal OP of both FNs and HNs with the corresponding to ϵ, where we use "UB" and "LB" to specify the upper and lower bounds, respectively.

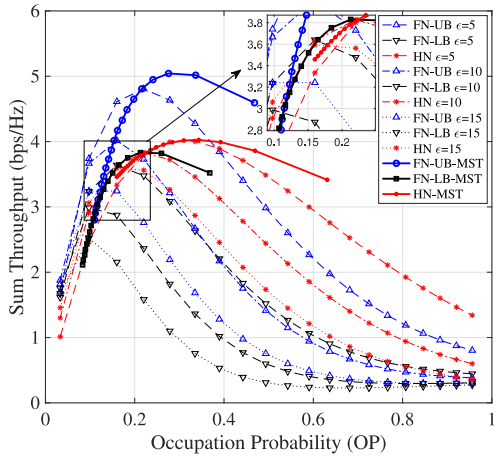

Fig. 8. The curves of sum throughput for both FNs and HNs as functions of OP with variant ϵ values, where we use "UB" and "LB" to specify the upper and lower bounds, respectively.

while it performs worse in HNs. This phenomenon is a good example of the performance gains brought by employing FNs.

In Fig. 8, the curves of the sum throughput for both FNs and HNs as functions of OP with variant ϵ values are illustrated, where the curves of the MST as well as the corresponding optimal OP for HNs (marked as HN-MST) together with the tight bounds of FNs corresponding to an ϵ value are also delineated. In particular, these three MST curves (from left to right) correspond to ϵ values from 20 dB to 1 dB. It is shown that the sum throughput of both FNs and HNs increase as ϵ increases if OP is not beyond their break-even points (e.g., OP is lower than 0.2) because the ACPs of both CLs and DLs in HNs/FNs are increasing, as shown in Fig. 7. However, if beyond their break points, the sum throughput of both FNs and HNs will decrease as ϵ increases following the decreases of ACP. Furthermore, the MST of both FNs and HNs are shown to be concave functions of ϵ, where HNs outperforms FNs in terms of MST while $\epsilon \geq 12$ dB. By employing the optimal OP, the MST of both FNs and HNs also have breakpoints in terms of ϵ, which implies that a well-chosen ϵ value is helpful to enhance the attainable best performance of both FNs and HNs. In summary, either a too-high or too-low ϵ value will erode the performance of the underlaying CNs, thus a proper ϵ value as well as an optimal OP value should be employed to optimize the sum throughput.

To more effectively optimize the sum throughput, the MST as well as the corresponding OP and ϵ value is analyzed, as illustrated in Fig. 9. The MST of both FNs and HNs is shown to be concave functions of ϵ. In particular, the FNs' MST is shown to decline faster than the HNs, implying that the HNs has a better MST performance while $\epsilon \geq 12$ dB. Furthermore, the corresponding optimal OP values of both FNs and HNs (marked as HN-OP) are shown to decrease rapidly at first as the SINR threshold increases, followed by slowly pace down and tend to be flat. In addition, HNs can afford a higher traffic workload, because the corresponding optimal OP of HNs is always higher than that of the FNs. Without considering the impact of SI, the corresponding optimal OP of HNs is always higher than that of the FNs, implying that HNs can afford more workload. In summary, although FNs can substantially outperform HNs in terms of the optimal MST, the former always fails to gain a benefit over the latter in terms of the affordable traffic workload.

D. Performance Comparison Between FN and HN in Terms of Both OP and the Activated Users

In this subsection, the number of ACUs and ADUs that sharing a sub-channel is assumed to be constant. Without loss of generality, we denote the number of the co-spectrum activated users by AUN. In particular, the SIC coefficient and the SINR threshold (i.e., μ and ϵ) are set to be moderate values 75 dB and 5 dB, respectively. The performance of the FNs/HNs in terms of OP and AUN is illustrated in Fig. 10-Fig. 12.

In Fig. 10, the ACP of both CLs and DLs as functions of OP with different AUN are analyzed. Compared with Fig. 3 and

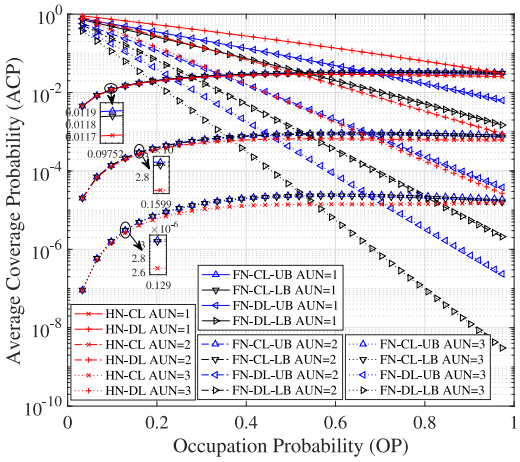

Fig. 10. The ACP-curves for both CL and DL as functions of OP with variant AUN in FNs/HNs, where we use "UB" and "LB" to specify the upper and lower bounds, respectively.

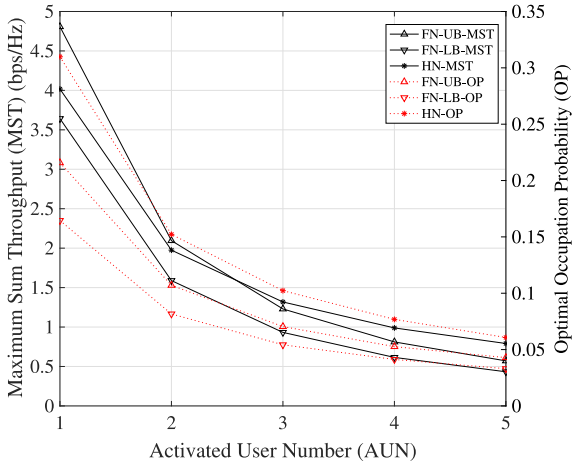

Fig. 12. The curves of the MST for both CL and DL as functions of OP with variant AUN in FNs/HNs, where we use "UB" and "LB" to specify the upper and lower bounds, respectively.

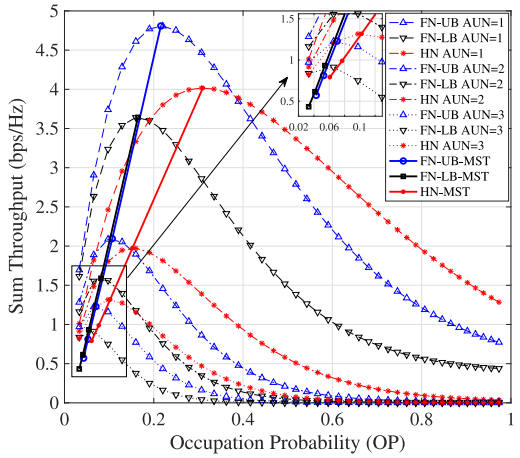

Fig. 11. The curves of sum throughput for both CL and DL as functions of OP with variant AUN in FNs/HNs, where we use "UB" and "LB" to specify the upper and lower bounds, respectively.

Fig. 7, an obvious performance loss is induced in CLs as AUN increases. In particular, the DLs shows the fastest decline rate among these three figures. Evidently, AUN will constitute the most critical parameter of the ACP performance of both CLs and DLs, because a severe interference will be imposed on CLs/DLs while more AU are accessed.

In Fig. 11, the curves of the sum throughput for both FNs and HNs as functions of OP with different AUN are illustrated, where the curves of the MST and the corresponding optimal OP for the upper and lower bounds of FNs/HNs with appropriate AUN are figured out. These three MST curves (from top to bottom) correspond to AUN values from 1 to 5. The sum throughput of both FNs and HNs are shown to substantially decline as AUN increases. Furthermore, if AUN is beyond 2, neither FNs nor HNs can afford a high data rate (e.g., OP ≥ 0.5) due to the fact that the sum throughput will tend to zero as OP increases. Compared with Fig. 5 and Fig. 8, the increasing of AUN is shown to be most unaffordable in both FNs and HNs under larger OP, since a small (but non-zero) sum throughput can be maintained as μ and ϵ increase, while almost zero sum throughput will be attained if AUN is beyond 2. In addition, the MST of both FNs and DNs are almost linearly decreasing as AUN increases, thus affording more AUN in a low-data-rate scenario in a cell of D2D-aided underlaying CNs. Anyway, less AUN can exist in the high-data-rate scenarios. In summary, the fewer the co-spectrum AUN, the greater the sum throughput that can be obtained, and vice versa.

To more effectively optimizing the sum throughput, the curves of the MST as well as the corresponding optimal OP for both FNs and HNs with a given AUN are analyzed, as illustrated in Fig. 12. It is shown that both the MST and the corresponding optimal OP decrease as AUN increases. Although HNs outperforms FNs in terms of MST when AUN is beyond 3, the affordable traffic volume has already declined to a very low value (since OP becomes less than 0.1). Thus we should share a sub-channel to as few AUs as possible for maximizing the sum throughput of the whole networks.

VIII. Conclusion

In this paper, the optimal mode selection (i.e., between FD and HD modes) in underlaying cellular networks was studied by taking the impact of the users' workload into account. The performance gains brought about by employing an appropriate duplex mode was substantially investigated. As the benchmarks, the closed-form expressions for a variety of critical parameters of metric under a given workload, including the average coverage probability, the sum throughput and the maximum sum throughput of FD/HD-D2D-aided underlaying cellular networks, etc, were derived and analyzed. It was shown that the FD mode is capable of improving the performance of the D2D-aided underlaying cellular networks in terms of sum throughput in the low-traffic-volume regime, while the HD mode won technical

advantage over the former in a high-traffic-volume regime. Furthermore, it is impossible for us to improve the sum throughput of D2D-aided underlaying cellular networks by simply increasing the users' traffic load indefinitely, in other words, there must be an optimal user workload to maximize the sum throughput of the entire system. By adaptively adjusting a variety of critical parameters, such as the traffic workload, the SINR threshold, the residual self-interference and the number of co-spectrum activated users, etc, the maximum sum throughput with optimal workload allocation can be attained.

APPENDIX A

The STP of CLs can be formulated:

$$\begin{aligned}\mathcal{S}_c^{(\mathrm{ND})} &= \mathbb{P}\left(\frac{\mathcal{P}_c h_{c_0b} d_{c_0b}^{-\alpha}}{I_{cc}+\sigma^2} > \epsilon\right) \\ &= \mathbb{P}\left[h_{c_0b} > \frac{\epsilon r_c^{\alpha}}{\mathcal{P}_c}(I_{cc}+\sigma^2)\right] \end{aligned} \tag{39}$$

where $r_c = d_{c_0b}$. It is shown in (39) that the STP probability depends on a number of variables, including h_{c_0b}, r_c, $\mathcal{P}_c$ and I_{cc}. Conditioning on $g = \{r_c, I_{cc}\}$, for a given transmit power $\mathcal{P}_c$, (39) can be rewritten as

$$\mathcal{S}_c^{(\mathrm{ND})} = \mathbb{E}_g\left(\mathbb{P}_g^{\mathrm{ND}}\right) \tag{40}$$

where the conditional probability $\mathbb{P}_g^{\mathrm{ND}}$ is given by:

$$\begin{aligned}\mathbb{P}_g^{\mathrm{ND}} &= \mathbb{P}\left[h_{c_0b} > \frac{\epsilon r_c^{\alpha}}{\mathcal{P}_c}(I_{cc}+\sigma^2)\right] \mid g \\ &\overset{(a)}{=} \int_{x=\frac{\epsilon r_c^{\alpha}}{\mathcal{P}_c}(I_{cc}+\sigma^2)}^{\infty} e^{-x}dx \\ &= e^{-s_c(I_{cc}+\sigma^2)} \end{aligned} \tag{41}$$

with $s_c = \epsilon r_c^{\alpha}/\mathcal{P}_c$. Since $h_{c_0b} \backsim \exp(1)$ holds, we can easily derive the expression in the step (a) following the the properties of exponential distribution. By substituting (41) into (40) and de-conditioning by g, both STP of CLs can be derived as:

$$\begin{aligned}\mathcal{S}_c^{(\mathrm{ND})} &= \mathbb{E}_g\left[e^{-s_c(I_{cc}+\sigma^2)}\right] \\ &= \mathbb{E}_{r_c}\left\{\mathbb{E}_{I_{cc}}\left[e^{-s_c(I_{cc}+\sigma^2)}\right]\right\} \\ &\overset{(b)}{=} \mathbb{E}_{r_c}\left[\mathcal{L}\left(s_c I_{cc}\right)e^{-s_c\sigma^2}\right] \\ &\overset{(c)}{=} \int_0^R \left[\mathcal{L}\left(s_c I_{cc}\right)e^{-s_c\sigma^2} f(r_c)\right] dr_c \end{aligned} \tag{42}$$

where in step (b), $\mathcal{L}(s_c I_{cc})$ denotes the Laplace transform (evaluated at s_c) of random variable I_{cc}. Moreover, in step (c), $f(r_c)$ stands for the probability density function of a randomly chosen CL.

APPENDIX B

Based on equations $\mathbb{E}[\prod_{\Phi} f(x)] = \exp\{-\lambda \int_{\mathbb{R}^2}[1 - f(x)]dx\}$ and $\int_{\mathbb{R}^2} f(x)dx = 2\pi\int_0^{\infty} x f(x)dx$, the Laplace transforms of I_{cc} can be given by

$$\begin{aligned}&\mathcal{L}\left(s_c I_{cc}\right) \\ &= \mathbb{E}_{(h,D)}\left\{\exp\left[-s_c\mathcal{P}_c\sum_{\Pi_c/c_0}\left(h_{c_ib}D_{c_ib}^{-\alpha}\right)\right]\right\} \\ &= \mathbb{E}_D\left[\prod_{\Pi_c/c_0}\left(\frac{1}{1+s_c\mathcal{P}_c D_{c_ib}^{-\alpha}}\right)\right] \\ &= \exp\left\{-2\pi\lambda_c\int_{r_c}^{\infty}\left(1-\frac{1}{1+s_c\mathcal{P}_c x^{-\alpha}}\right)xdx\right\} \\ &= \exp\left\{-2\pi\lambda_c\int_{r_c}^{\infty}\left(\frac{1}{1+\frac{x^{\alpha}}{\epsilon r^{\alpha}}}\right)xdx\right\} \\ &= \exp\left\{-2\pi\lambda_c\int_{\epsilon^{-1}}^{\infty}\frac{r_c^2\epsilon^{\frac{2}{\alpha}}u^{\frac{2}{\alpha}-1}}{1+u}du\right\} \\ &= \exp\left\{-2\pi\lambda_c\frac{r_c^2\epsilon}{(1-\frac{2}{\alpha})^2}({}_2F_1)\left(1,1-\frac{2}{\alpha};2-\frac{2}{\alpha};-\epsilon\right)\right\} \\ &= \exp\left[-2\pi\lambda_c r_c^2\rho(\alpha,\epsilon)\right] \end{aligned} \tag{43}$$

where $u = x^{\alpha}/(\epsilon r_c^{\alpha})$ and $\rho(\alpha,\epsilon) = \frac{\epsilon}{(1-\frac{2}{\alpha})^2}({}_2F_1)(1,1-\frac{2}{\alpha};2-\frac{2}{\alpha};-\epsilon)$. Note that the integral region in the above equation is (r_c,∞), because users are assumed to always choose the nearest BS as their access point (i.e., to guarantee the maximum received signal strength). In this case, the distance between the interfering BS and the target user is always greater than the distance r_c.

APPENDIX C

The Laplace transforms of $I_{dd}^{(\mathrm{FD})}$ can be given by

$$\begin{aligned}&\mathcal{L}\left(s_d I_{dd}^{(\mathrm{FD})}\right) \\ &= \mathbb{E}_D\left[\prod_{\Pi_d/x_0}\left(\frac{1}{1+s_d\mathcal{P}_d d_{x_id}^{-\alpha}}\frac{1}{1+s_d\mathcal{P}_d d_{m(x_i)d}^{-\alpha}}\right)\right] \\ &= \exp\left\{-2\pi\lambda_d\int_0^{\infty}\left(1-\frac{1}{1+s_d\mathcal{P}_d x^{-\alpha}}\right.\right. \\ &\qquad\left.\left.\cdot\frac{1}{1+s_d\mathcal{P}_d\parallel x+R_d(\cos\varphi_i,\sin\varphi_i))\parallel^{-\alpha}}\right)xdx\right\} \\ &= \exp\left\{-2\pi\lambda_d\int_0^{\infty} g(s_d,x,R_d,\varphi)xdx\right\} \end{aligned} \tag{44}$$

where

$$\begin{aligned}&g(s,x,r_d,\varphi) \\ &= 1-\frac{1}{1+s\mathcal{P}_d x^{-\alpha}}\frac{1}{1+s\mathcal{P}_d\left\|x+R_d\left(\cos\varphi_i,\sin\varphi_i\right)\right\|^{-\alpha}}. \end{aligned}$$

APPENDIX D

Based on the FKG inequality [37], the lower bound of $\mathcal{L}(s_d I_{dd}^{(\mathrm{FD})})$ can be formulated by

$$\begin{aligned}
&\mathcal{L}\left(s_d I_{dd}^{(\mathrm{FD})}\right) \\
&= \mathbb{E}_D\left[\prod_{\Pi_d/x_0}\left(\frac{1}{1+s_d\mathcal{P}_d D_{x_i d}^{-\alpha}}\frac{1}{1+s_d\mathcal{P}_d D_{m(x_i)d}^{-\alpha}}\right)\right] \\
&\geq \mathbb{E}_D\left[\prod_{\Pi_d/x_0}\frac{1}{1+s_d\mathcal{P}_d D_{x_i d}^{-\alpha}}\right]\mathbb{E}_D\left[\prod_{\Pi_d/x_0}\frac{1}{1+s_d\mathcal{P}_d D_{m(x_i)d}^{-\alpha}}\right] \\
&= \exp\left[-2\pi\lambda_d R_d^2\epsilon^{\frac{2}{\alpha}}\frac{2\pi}{\alpha\sin\left(\frac{2\pi}{\alpha}\right)}\right] \\
&= \exp\left[-2\pi\lambda_d R_d^2\delta(\alpha,\epsilon)\right] \qquad (45)
\end{aligned}$$

Based on the Cauchy-Schwarz inequality, the upper bound of $\mathcal{L}(s_d I_{dd}^{(\mathrm{FD})})$ can be derived:

$$\begin{aligned}
&\mathcal{L}\left(s_d I_{dd}^{(\mathrm{FD})}\right) \\
&= \mathbb{E}_D\left[\prod_{\Pi_d/x_0}\left(\frac{1}{1+s_d\mathcal{P}_d D_{x_i d}^{-\alpha}}\frac{1}{1+s_d\mathcal{P}_d D_{m(x_i)d}^{-\alpha}}\right)\right] \\
&\leq \left\{\mathbb{E}_D\left[\prod_{\Pi_d/x_0}\left(\frac{1}{1+s_d\mathcal{P}_d D_{x_i d}^{-\alpha}}\right)^2\right]\right. \\
&\quad \left.\cdot\,\mathbb{E}_D\left[\prod_{\Pi_d/x_0}\left(\frac{1}{1+s_d\mathcal{P}_d D_{m(x_i)d}^{-\alpha}}\right)^2\right]\right\}^{\frac{1}{2}} \\
&= \exp\left[-\left(1+\frac{2}{\alpha}\right)\pi\lambda_d R_d^2\epsilon^{\frac{2}{\alpha}}\frac{2\pi}{\alpha\sin\left(\frac{2\pi}{\alpha}\right)}\right] \\
&= \exp\left[-\left(1+\frac{2}{\alpha}\right)\pi\lambda_d R_d^2\delta(\alpha,\epsilon)\right] \qquad (46)
\end{aligned}$$

REFERENCES

[1] Z. Zhang, K. Long, J. Wang, and F. Dressler, "On swarm intelligence inspired self-organized networking: Its bionic mechanisms, designing principles, and optimization approaches," *IEEE Commun. Surv. Tut.*, vol. 16, no. 1, pp. 513–537, Jan.-Mar. 2014.

[2] S. Chen, Q. Fei, H. Bo, L. Xi, and Z. Chen, "User-centric ultra-dense networks for 5G: Challenges, methodologies, and directions," *IEEE Wireless Commun.*, vol. 23, no. 2, pp. 78–85, Apr. 2016.

[3] S. Chen and Z. Jian, "The requirements, challenges, and technologies for 5G of terrestrial mobile telecommunication," *IEEE Commun. Mag.*, vol. 52, no. 5, pp. 36–43, May 2014.

[4] Z. Zhang, K. Long, and J. Wang, "Self-organization paradigms and optimization approaches for cognitive radio technologies: A survey," *IEEE Wireless Commun.*, vol. 20, no. 2, pp. 36–42, Apr. 2013.

[5] Y. Chen, X. Ji, K. Huang, B. Li, and X. Kang, "Opportunistic access control for enhancing security in D2D-enabled cellular networks," *Sci. China Inf. Sci.*, vol. 61, no. 4, pp. 187–198, 2018.

[6] C. Xing, M. Ying, Y. Zhou, and F. Gao, "Transceiver optimization for multi-hop communications with per-antenna power constraints," *IEEE Trans. Signal Process.*, vol. 64, no. 6, pp. 1519–1534, Mar. 2016.

[7] K. Yang, N. Yang, N. Ye, M. Jia, Z. Gas, and R. Fan, "Non-orthogonal multiple access: Achieving sustainable future radio access," *IEEE Commun. Mag.*, vol. 57, no. 2, pp. 116–121, Feb. 2019.

[8] J. An, K. Yang, J. Wu, N. Ye, S. Guo, and Z. Liao, "Achieving sustainable ultra-dense heterogeneous networks for 5G," *IEEE Commun. Mag.*, vol. 55, no. 12, pp. 84–90, Dec. 2017.

[9] M. Naslcheraghi, M. Afshang, and H. S. Dhillon, "Modeling and performance analysis of full-duplex communications in cache-enabled D2D networks," in *Proc. IEEE Int. Conf. Commun.*, May 2018, Art. no. 17971794.

[10] Z. Liu, P. Tao, P. Bo, and W. Wang, "Sum-capacity of D2D and cellular hybrid networks over cooperation and non-cooperation," in *7th Int. Conf. Commun. Netw.*, China, Kun Ming, 2012, pp. 707–711.

[11] A. A. A. Haija and V. Mai, "Spectral efficiency and outage performance for hybrid D2D-infrastructure uplink cooperation," *IEEE Trans. Wireless Commun.*, vol. 14, no. 3, pp. 1183–1198, Mar. 2015.

[12] C. Xu, P. Zeng, W. Liang, and H. Yu, "Secure resource allocation for green and cognitive device-to-device communication," *Sci. China Inf. Sci.*, vol. 61, no. 2, Nov. 2017, Art. no. 029305.

[13] J. Liu, S. Zhang, H. Nishiyama, N. Kato, and J. Guo, "A stochastic geometry analysis of D2D overlaying multi-channel downlink cellular networks," in *Proc. IEEE Conf. Comput. Commun.*, Kowloon, 2015, pp. 46–54.

[14] G. Fodor *et al.*, "Design aspects of network assisted device-to-device communications," *IEEE Commun. Mag.*, vol. 50, no. 3, pp. 170–177, Mar. 2012.

[15] R. Zhang, Y. Li, C.-X. Wang, Y. Ruan, and H. Zhang, "Energy efficient power allocation for underlaying mobile D2D communications with peak/average interference constraints," *Sci. China Inf. Sci.*, vol. 61, no. 8, Mar. 2018, Art. no. 089301.

[16] H. Chen, L. Liu, H. S. Dhillon, and Y. Yi, "QoS-aware D2D cellular networks with spatial spectrum sensing: A stochastic geometry view," *IEEE Trans. Commun.*, vol. 67, no. 5, pp. 3651–3664, May 2019.

[17] L. Lei, Y. Kuang, X. Shen, C. Lin, and Z. Zhong, "Resource control in network assisted device-to-device communications: Solutions and challenges," *IEEE Commun. Mag.*, vol. 52, no. 6, pp. 108–117, Jun. 2014.

[18] K. S. Ali, H. ElSawy, and M. Alouini, "Modeling cellular networks with full-duplex D2D communication: A stochastic geometry approach," *IEEE Trans. Commun.*, vol. 64, no. 10, pp. 4409–4424, Oct. 2016.

[19] Z. Zhang, K. Long, A. V. Vasilakos, and L. Hanzo, "Full-duplex wireless communications: Challenges, solutions, and future research directions," *Proc. IEEE*, vol. 104, no. 7, pp. 1369–1409, Jul. 2016.

[20] Z. Zhang, X. Chai, K. Long, and A. V. Vasilakos, "Full duplex techniques for 5G networks: Self-interference cancellation, protocol design, and relay selection," *IEEE Commun. Mag.*, vol. 53, no. 5, pp. 128–137, May 2015.

[21] B. Zhong and Z. Zhang, "Opportunistic two-way full-duplex relay selection in underlay cognitive networks," *IEEE Syst. J.*, vol. 12, no. 1, pp. 725–734, Mar. 2018.

[22] D. Feng, L. Lu, Y. W. Yi, and G. Li, "Device-to-device communications in cellular networks," *IEEE Commun. Mag.*, vol. 52, no. 4, pp. 49–55, Apr. 2016.

[23] H. Min, J. Lee, S. Park, and D. Hong, "Capacity enhancement using an interference limited area for device-to-device uplink underlaying cellular networks," *IEEE Trans. Wireless Commun.*, vol. 10, no. 12, pp. 3995–4000, Dec. 2011.

[24] C. Ma, J. Liu, X. Tian, Y. Hui, C. Ying, and X. Wang, "Interference exploitation in D2D-enabled cellular networks: A secrecy perspective," *IEEE Trans. Commun.*, vol. 63, no. 1, pp. 229–242, Jan. 2015.

[25] W. Li, T. Fei, T. Svensson, D. Feng, and S. Li, "Exploiting full duplex for device-to-device communications in heterogeneous networks," *IEEE Commun. Mag.*, vol. 53, no. 5, pp. 146–152, May 2015.

[26] H. A. Mustafa, M. Z. Shakir, M. A. Imran, A. Imran, and R. Tafazolli, "Coverage gain and device-to-device user density: Stochastic geometry modeling and analysis," *IEEE Commun. Lett.*, vol. 19, no. 10, pp. 1742–1745, Oct. 2015.

[27] N. Lee, X. Lin, J. G. Andrews, and R. W. Heath, "Power control for D2D underlaid cellular networks: Modeling, algorithms, and analysis," *IEEE J. Sel. Areas Commun.*, vol. 33, no. 1, pp. 1–13, Jan. 2015.

[28] J. G. Andrews, F. Baccelli, and R. K. Ganti, "A tractable approach to coverage and rate in cellular networks," *IEEE Trans. Commun.*, vol. 59, no. 11, pp. 3122–3134, Nov. 2011.

[29] Y. Zhou, L. Hang, Z. Pan, T. Lin, J. Shi, and G. Yang, "Two-stage cooperative multicast transmission with optimized power consumption and guaranteed coverage," *IEEE J. Sel. Areas Commun.*, vol. 32, no. 2, pp. 274–284, Feb. 2014.

[30] Z. Liu, P. Tao, Q. Lu, and W. Wang, "Transmission capacity of D2D communication under heterogeneous networks with dual bands," in *Proc. Int. ICST Conf. Cognitive Radio Oriented Wireless Netw. Commun.*, Stockholm, 2012, pp. 169–174.

[31] S. Jian *et al.*, "Optimal mode selection with uplink data rate maximization for D2D-aided underlaying cellular networks," *IEEE Access*, vol. 4, no. 99, pp. 8844–8856, Nov. 2016.
[32] X. Chai, L. Tong, C. Xing, H. Xiao, and Z. Zhang, "Throughput improvement in cellular networks via full-duplex based device-to-device communications," *IEEE Access*, vol. 4, pp. 7645–7657, Oct. 2016.
[33] N. Haider, A. Ali, C. Suarez-Rodriguez, and E. Dutkiewicz, "Optimal mode selection for full-duplex enabled D2D cognitive networks," *IEEE Access*, vol. 7, pp. pp. 57298–57311, May 2019.
[34] H. Lee, D. Kim, and D. Hong, "Mode selection in multi-user full-duplex systems considering inter-user interference," in *Proc. 24th Eur. Signal Process. Conf.*, Aug. 2016, pp. 769–772.
[35] S. Lien, C. Chien, G. S. Liu, H. Tsai, R. Li, and Y. J. Wang, "Enhanced LTE device-to-device proximity services," *IEEE Commun. Mag.*, vol. 54, no. 12, pp. 174–182, Dec. 2016.
[36] I. S. Gradshteyn and I. M. Ryzhik, *Table of Integrals, Series, and Product*, 5th ed. Boston: Academic Press, 1994.
[37] S. N. Chiu, D. Stoyan, W. Kendall, and J. Mecke, *Stochastic Geometry and Its Applications*, 3rd ed. Wiley, Aug. 2013.

Changhao Du received the B.E. degree from the Beijing University of Chemical Technology, Beijing, China, in 2009, and the M.S. and Ph.D. degrees from the Beijing Institute of Technology, Beijing, China, in 2012 and 2018, respectively. From October 2016 to October 2017, he was a Visiting Ph.D. Student with the Chalmers University of Technology, Sweden, under the financial support of China Scholarship Council. Since July 2018, he has been with the Beijing University of Posts and Telecommunications, China, as a Postdoctoral Research Associate. His research interest include statistical signal processing, applied signal processing and physical layer of wireless communication systems, including D2D communications, GPS navigation, laser and THz communications, channel estimation, and synchronization.

Zhongshan Zhang (Senior Member, IEEE) received the B.E. and M.S. degrees in computer science from the Beijing University of Posts and Telecommunications (BUPT), Beijing, China, in 1998 and 2001, respectively, and the Ph.D. degree in electrical engineering from BUPT, in 2004. From August 2004, he joined DoCoMo Beijing Laboratories as an Associate Researcher, and was promoted to a Researcher in December 2005. From February 2006, he joined the University of Alberta, Edmonton, AB, Canada, as a Postdoctoral Fellow. From April 2009, he joined the Department of Research and Innovation (R&I), Alcatel-Lucent, Shanghai, as a Research Scientist. From August 2010 to July 2011, he worked in NEC China Laboratories, as a Senior Researcher. He has been serving as a Guest Editor and an Editor for several technical journals, such as the *IEEE Communications Magazine* and *KSII Transactions on Internet and Information Systems*. He is currently a Professor with the School of Communication and Electronics, Beijing Institute of Technology, Beijing, China. His main research interests include statistical signal processing, self-organized networking, cognitive radio, and cooperative communications.

Xiaoxiang Wang received the B.S degree in physics from Qufu Normal University, Qufu, China, in 1991, the M.S. degree in information engineering from East China Normal University, Shanghai, China, in 1994, and the Ph.D. degree in electronic engineering from the Beijing Institute of Technology, Beijing, China, in 1998. In 1998, she joined the School of Information and Communication Engineering, Beijing University of Posts and Telecommunications. She was a Visiting Scholar with the Vienna University of Technology from 2001 to 2002. From August 2010 to February 2011, she was a Visiting Fellow with the Department of Electrical and Computer Engineering, North Carolina State University, Raleigh. Her research interests include communications theory and signal processing, with specific interests in cooperative communications, multiple-input-multiple-output systems, multimedia broadcast/multicast service systems, and resource allocation.

Jianping An (Member, IEEE) received the B.E. degree from Information Engineering University in 1987, and the M.S. and Ph.D. degrees from the Beijing Institute of Technology, Beijing, China, in 1992 and 1996, respectively. Since 1996, he has been with the School of Information and Electronics, Beijing Institute of Technology, where he now holds the post of Full Professor. From 2010 to 2011, he was a Visiting Professor with the University of California, San Diego. He has authored more than 150 journal and conference articles and holds (or co-holds) more than 50 patents. His current research interest is focused on digital signal processing theory and algorithms for communication systems. He was the recipient of various awards for his academic achievements and the resultant industrial influences, including the National Award for Scientific and Technological Progress of China (1997) and the Excellent Young Teacher Award by the China's Ministry of Education (2000). Since 2010, he has been serving as a Chief Reviewing Expert for the Information Technology Division, National Scientific Foundation of China.